

# Interstellar Meteoroids

Mária Hajduková Jr., Veerle Sterken and Paul Wiegert

## 10.1 Introduction

Meteor observations provide us with primary information about the meteoroid population in our Solar System, and address the important question of the origin of these meteoroids. Dust particles, larger grains, and fragments produced by collisions and disintegration processes are subject to gravitational and non-gravitational forces, which cause their dynamical and physical evolution and which can obscure their place and time of origin. This chapter is dedicated to those particles which arrive from outside the Solar System and to the problem of distinguishing them from local meteoroids.

The question of the origin of meteoroids, and in particular, the fraction of interstellar particles in the Solar System, has been a matter of long debate. The reason for this has been the abundance of hyperbolic orbits among detected meteors, as a hyperbolic excess above the escape velocity with respect to the Sun indicates a possible interstellar origin. In fact, a hyperbolic orbit is the only easily measurable property of a meteoroid that might indicate an interstellar origin, and so speed measurements are central to this discussion.

How much of the dust population originates locally in the Solar System and how much comes from beyond? How big is the probability that an interstellar particle passing through the Solar System will hit the Earth? How are the speed measurements by which interstellar meteoroids are identified affected by the uncertainties of the statistical treatment or the measurement errors?

In the first part of this chapter, we introduce interstellar particles from a theoretical point of view, describing their dynamical behaviour, orbital characteristics and their expected velocities measured at Earth. We examine the possible sources of the hyperbolicity of the meteoroid's orbit and demonstrate the problem of distinguishing the particles of interstellar origin from those produced in the Solar System or caused by the process of measuring. The second part of this chapter deals with experimental results based on Earth-based and space-borne observations. These have given rise to many searches within the last twenty-five years, the main results of which are summarised here and linked to the historical context.

### 10.1.1 Historical Background

During the first half of the twentieth century, the general opinion, influenced mostly by the work of Hoffmeister and Öpik, was that the majority of meteors are produced by interstellar particles. This finding was based on the results of visual meteor

observations and estimates of the meteor angular velocities. In the 1925 catalogue of visual fireballs measurements (Von Nießl and Hoffmeister, 1925), 79 percent of the meteors listed had hyperbolic orbits with respect to the Sun.

In the years 1931–1933, the Harvard Observatory organised the Arizona Expedition, the results of which supported this attitude. From rocking-mirror visual observations of angular velocities, Öpik (1940) concluded that about 60% of sporadic meteors were moving in hyperbolic orbits, with heliocentric velocities in excess of the parabolic limit, and defended their interstellar origin on a long-term basis (Öpik, 1950). Not until nearly thirty years later (Öpik, 1969) did he concede that the analysis of the velocities (not their observations) in the Arizona results was faulty and declared that the high fraction of hyperbolic meteors found by Öpik (1940) did not exist, proposing the true fraction of hyperbolic orbits was under 1%.

The theory of the predominance of the interstellar meteoroids over local interplanetary ones became indefensible with the progress of observational techniques and consequent improvements in velocity determination; mainly with double-camera photography and direct velocity measurements using the rotating shutter method.

Based on the first photographic observations, Whipple (1940) found that Hoffmeister's most significant interstellar stream was in fact associated with the comet Encke, a definitely local source with one of the shortest periods of all known comets and an aphelion in the asteroid belt.

Porter (1944), analysing British visual meteor data, found no direct evidence for the existence of an excess of hyperbolic velocities. He declared that, with a few doubtful exceptions, all meteors in his sample were members of the Solar System and pointed out the lack of any systematic analysis of the meteor data of the Arizona observations.

The new radio-echo techniques for velocity measurements, developed after 1945, brought the following results in the study of hyperbolic meteors: McKinley (1951), analysing thousands of meteor velocities in the records from the Ottawa radar, did not find one that he could definitely assert to be a meteor from interstellar space; radar meteor observations from Jodrell Bank (Almond et al., 1953) showed no evidence of a significant hyperbolic velocity component either.

Summarising the results obtained by different techniques, Lovell (1954) sceptically suggested that if any of the observed hyperbolic meteors were real, their possible origin was in planetary perturbations.

The final breakthrough was brought about by precise photographic observations at the Smithsonian Astrophysical

Observatory (the Harvard Super-Schmidt photographic program), the results of which were published by Jacchia and Whipple (1961). Their data contained so few hyperbolic orbits that they announced that there were statistically hardly any hyperbolic meteors.

In the following years, research into hyperbolic meteors, and especially interstellar meteoroids, focused on the determination of their ratio in the population of observed meteors. Štohl (1970) studied the hyperbolicity of meteors and also investigated the effect of planetary perturbations on meteoroid orbits. Comparing the results of the photographic catalogues collected until 1970, he found large differences in the percentage of hyperbolic orbits (from less than 2% to more than 20%) and showed the percentage clearly depended on the accuracy of the speed measurement.

Analyses of the Kharkov radar data (Tkachuk and Kolomiets, 1985; Andreev et al., 1987) yielded 1–2% hyperbolic orbits among more precise radar orbits and 5% for orbits of lower accuracy. The authors pointed out a lack of criteria for distinguishing real hyperbolic orbits.

Sarma and Jones (1985) reported 19% apparent hyperbolic orbits in their double-station video meteor data, of which 26 (6%) were hyperbolic on the basis of 95% confidence limits and only 8 (1.7%) were regarded as truly hyperbolic after considering the uncertainties arising from difficulties with the velocity determination.

Hajduková (1993), analysing photographic orbits collected in the IAU Meteor Data Centre, determined that the ratio of hyperbolic orbits in the data shrank considerably from 12% to 0.02% after a detailed error analysis. She concluded that there is no evidence for meteors of interstellar origin in the photographic surveys and that the hyperbolic velocities observed at Earth are most likely the consequence of observational and measurement errors, mostly in the velocity.

A new period in the research of interstellar meteoroids started with the first in situ measurements of interstellar dust by detectors, mainly on board the Ulysses and Galileo spacecraft. Research moved towards particles of smaller sizes, typically less than 1  $\mu\text{m}$ , and too small to be detected as meteors at the Earth, but measurable with space-borne dust detectors. Grün and his colleagues (Grün et al., 1993) confidently reported the identification of interstellar dust (ISD) grains flowing through the heliosphere, originating from the Local Interstellar Cloud (LIC). They reported that small dust impacts can be clearly distinguished from noise for most of the events due to the multi-coincidence characteristics of the instrument of the detector (Baguhl et al., 1993).

Around the same time, Baggaley et al. (1993a), on the basis of observations from the Advanced Meteor Orbit Radar, dealt with the influx of meteoroids with extremely high velocities. Their work and other related measurements are discussed more fully in Section 10.5.2.1.

From this point, monitoring of the influx of interstellar particles (ISP) by various techniques in the following years enabled tens of papers about their detection to be published. These have brought valuable information about the number of interstellar particles registered by various techniques, which depend on their distance from the Sun, their location (near ecliptic planetary regions or in high ecliptic latitudes) and on their size.

### 10.1.2 Significance of Interstellar Meteoroid Detections

This topic of debate is important because a conclusive detection of interstellar meteoroids from radar measurements would have significant consequences for astronomy. Although the size distribution of the interstellar dust particles declines exponentially with the particle size, the mass distribution is dominated by large particles (Landgraf et al., 2000), e.g., larger than about 1  $\mu\text{m}$ . Therefore, a reliable detection of a large-ISD-particle flux would considerably change the interstellar gas-to-dust mass ratio. The most recent gas-to-dust mass ratio – derived from in situ dust measurements of particles from the LIC by the Ulysses spacecraft – was determined to be  $R_{g/d} = 193^{+85}_{-57}$  (Krüger et al., 2015). For this number, a dust inflow velocity of  $v_{\infty} = 23.2 \text{ km s}^{-1}$  was assumed. The gas-to-dust mass ratio is about 20% higher when assuming  $v_{\infty} = 26 \text{ km s}^{-1}$  (Krüger et al., 2015).

Moreover, the presence of large interstellar particles and their characterisation would provide more information on the processes taking place in interstellar space like collisions, shocks and mixing. Several consequences, like a non-homogeneous distribution of the dust in the interstellar medium, are discussed in Grün and Landgraf (2000).

Finally, detection and analysis of large interstellar dust fluxes or interstellar meteors may, for the first time, permit the study of debris disks from other stars from observations of dust in the Solar System, complementing astronomical observations. This is not possible using smaller (micron-sized) interstellar dust particles from spacecraft in situ data since they do not directly represent their source region (see Section 10.2). Interstellar meteoroids could thus provide unique information, because in situ measurements, sample return missions and astronomical observations often have limitations in their ability to detect these large grains.

## 10.2 Dynamics of Extra-Solar System Particles

Interstellar dust in the heliosphere may come from different sources in our local galactic neighbourhood via different ejection mechanisms (see Section 10.3), but one confirmed source of interstellar dust is the Local Interstellar Cloud (LIC) through which the Sun currently moves with a relative speed of about  $26 \text{ km s}^{-1}$ , in the direction of the neighbouring G-cloud. The Local Interstellar Cloud is a dense ( $0.3 \text{ H cm}^{-3}$ ; Frisch et al., 1999), warm, partially ionised cloud consisting of H and He gas and about 0.5–1% dust by mass. The LIC is embedded in a low density region of space called the *Local Bubble* that was likely excavated by a few supernovae. The dust in the LIC is coupled to its magnetic fields on distance scales of  $\sim 0.06 \text{ pc}$  (for a 1  $\mu\text{m}$  particle radius) to  $\sim 6 \text{ pc}$  for a 10  $\mu\text{m}$  particle radius (assuming particle material density  $\rho = 1000 \text{ kg m}^{-3}$ ), because they are charged and move through the Local Interstellar Magnetic Field (Grün and Svestka, 1996)<sup>1</sup>. Their surface equilibrium potential is estimated to be about +5 or +12 V for

<sup>1</sup> The LIC is about 9 pc in size. Table 10.1 shows the gyroradii in the LIC for various particle sizes.

Table 10.1. Particle masses (in kg) with corresponding radii for different particle bulk material densities ( $\rho$  in  $\text{g cm}^{-3}$ ).  $\beta$  (ratio of solar radiation pressure to gravity for a dust particle) and  $Q/m$  (charge-to-mass ratio of a dust particle) are calculated assuming the “adapted astronomical silicates  $\beta$ -curve” and a bulk material density of  $2.5 \text{ g cm}^{-3}$ . The Gyroradius in the Local Interstellar Cloud is given for particle surface potential  $U = +0.5 \text{ V}$ , interstellar magnetic field strength  $B = 0.5 \text{ nT}$  and particle bulk material density  $\rho = 2.5 \text{ g cm}^{-3}$

Mass [kg]	$\rho = 3.3$	$\rho = 2.5$	$\rho = 0.7$	$\beta[-]$	$Q/m [\text{C kg}^{-1}]$	Gyroradius
	Radius	Radius	Radius			
	[mm]	[mm]	[mm]			[pc]
1.	41.67	45.71	69.87	0.	$2.5 \times 10^{-11}$	$8.5 \times 10^7$
$10^{-1}$	19.34	21.21	32.42	0.	$1.2 \times 10^{-10}$	$1.8 \times 10^7$
$10^{-2}$	8.98	9.85	15.05	0.	$5.5 \times 10^{-10}$	$3.9 \times 10^6$
$10^{-3}$	4.16	4.57	6.99	0.	$2.5 \times 10^{-09}$	$8.5 \times 10^5$
$10^{-4}$	1.93	2.12	3.24	0.	$1.2 \times 10^{-08}$	$1.8 \times 10^5$
	[ $\mu\text{m}$ ]	[ $\mu\text{m}$ ]	[ $\mu\text{m}$ ]			
$10^{-5}$	898	985	1505	0.	$5.5 \times 10^{-08}$	$3.9 \times 10^4$
$10^{-6}$	417	458	699	0.	$2.5 \times 10^{-07}$	$8.5 \times 10^3$
$10^{-7}$	193	212	324	0.	$1.2 \times 10^{-06}$	$1.8 \times 10^3$
$10^{-8}$	89.8	98.5	150.5	0.	$5.5 \times 10^{-06}$	395
$10^{-9}$	41.7	45.7	69.9	0.006	$2.5 \times 10^{-05}$	82
$10^{-10}$	19.3	21.2	32.4	0.01	$1.2 \times 10^{-05}$	18
$10^{-11}$	8.98	9.85	15.05	0.03	$5.5 \times 10^{-04}$	3.9
$10^{-12}$	4.17	4.57	6.97	0.07	$2.5 \times 10^{-03}$	0.82
						[AU]
$10^{-13}$	1.93	2.12	3.24	0.15	$1.2 \times 10^{-02}$	$3.7 \times 10^4$
$10^{-14}$	0.89	0.98	1.60	0.36	$5.5 \times 10^{-02}$	$8.1 \times 10^3$
$10^{-15}$	0.42	0.46	0.70	0.88	0.25	$1.8 \times 10^3$
$10^{-16}$	0.19	0.21	0.32	1.54	1.2	371
$10^{-17}$	0.09	0.10	0.15	1.29	5.5	81
$10^{-18}$	0.04	0.05	0.07	0.50	25.4	18

silicate and graphite grains respectively in the Local Bubble, and +0.5 to +1 V in the local interstellar cloud (Grün and Svstka, 1996). The surface equilibrium potential increases to +2–+3 V (Alexashov et al., 2016) or +8–+10 V (Slavin et al., 2012) in the outer boundary regions of the heliosphere, with the consequence that large particles can penetrate freely into the heliosphere, while smaller ones are prevented from entering the heliosphere and are deflected around it instead. Linde and Gombosi (2000) calculated the filtering of dust at the heliospheric boundary and concluded that particles between 0.1 and 0.2  $\mu\text{m}$  are filtered out. This seemed somewhat pessimistic and was based on a defocusing configuration of the heliospheric magnetic fields. Slavin et al. (2012) found that particles smaller than 0.01  $\mu\text{m}$  are completely excluded from the heliosphere.

Once the interstellar dust moves inside the heliosphere, it is also subject to forces that influence its trajectories and that may even prevent it from reaching the Solar System. The most important of these forces are solar gravity, the solar radiation pressure force and the Lorentz force due to the motion of the charged dust particles in the Interplanetary Magnetic Field (IMF). Other forces like solar wind drag, Coulomb drag, or Poynting–Robertson drag and the Yarkovsky effect play a negligible role for ISD (Altobelli, 2004). We assume that there is no mass loss for the particles.

The solar radiation pressure and gravity both depend on the square distance to the Sun, and hence, can be written in one

term  $\beta = F_{SRP}/F_{grav}$  that depends on the grain composition, morphology, particle size, density and on the solar radiation. The relation between the particle size and  $\beta$ -value is visualised in a so-called  $\beta$ -curve. Figure 10.1 shows such curves for different materials. “Astronomical silicates” (see Figure 10.1) are hypothetical silicates, with for instance inclusions or mantles, that have optical constants consistent with the astronomical observations of interstellar silicates (Draine and Lee, 1984).

ISD particles with  $\beta = 1$  move straight through the Solar System without being perturbed by solar gravity or the radiation pressure force. Particles with  $\beta > 1$  decelerate when approaching the Sun, and then accelerate again on their hyperbolic orbit into interstellar space. Such particles typically have diameters between about 0.2 and 0.6  $\mu\text{m}$  for silicates (see Figure 10.1, around  $\sim 8 \times 10^{-18} \text{ kg}$  and  $2 \times 10^{-16} \text{ kg}$ ). On the contrary, particles with  $\beta < 1$  (diameters larger than about one micron) accelerate near the Sun and then slow down again to continue on their hyperbolic trajectories into interstellar space (Sterken et al., 2012, Fig. 1–3). Particles with  $\beta < 1$  can reach speeds of up to 40  $\text{km s}^{-1}$  at Earth’s distance from the Sun, instead of the undisturbed 26  $\text{km s}^{-1}$  for particles from the LIC of about 1.5  $\mu\text{m}$  diameter (Strub et al., 2019). The largest particles reach speeds up to 49  $\text{km s}^{-1}$  (heliocentric velocity). The gravitational focusing from the Sun causes a region of higher interstellar dust number density to be located “downstream” from the Sun (Landgraf, 2000). The number density there increases up to a factor

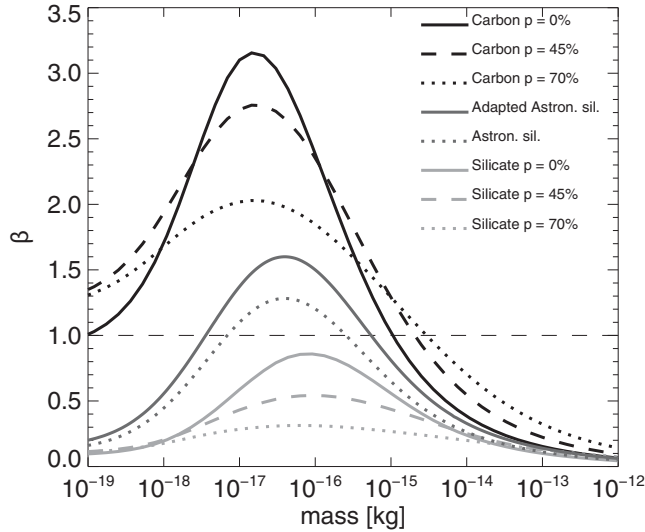


**Figure 10.1.** The  $\beta$ -mass relation for several particle sizes and material properties. Porosity  $p$  is the ratio of the volume of void space to the total (bulk) material space of the particle. Porosity  $p = 0\%$  corresponds to compact material. Credit: adapted from Kimura and Mann (1999) and Sterken et al. (2012), reproduced with permission © ESO and the Astronomical Institute of the Slovak Academy of Sciences. (A black and white version of this figure will appear in some formats. For the colour version, please refer to the plate section.)

of 5 (for LIC particles) at Earth’s distance from the Sun, and depending on particle size. The Earth passes this enhanced-density region of (large) dust from the LIC every year, around December 13 (Strub et al., 2019).

On the contrary, particles with  $\beta > 1$  create a void region around the Sun, called the “ $\beta$ -cone” where these particles with  $\beta > \beta_{\text{cone}}$  cannot enter. Since the Earth is within the  $\beta$ -cone for  $\beta = 1.4$ , interstellar dust with  $\beta > 1.4$  cannot be detected from 1 AU (Strub et al., 2019). Only particles smaller than about 0.3  $\mu\text{m}$  in diameter or larger than about 0.6  $\mu\text{m}$  in diameter (assuming the adapted astronomical silicates  $\beta$ -curve; see Figure 10.1) can be detected locally near the Earth (Strub et al., 2019). Particles between 0.3 and 0.6  $\mu\text{m}$  in diameter are in the size range of the bulk of the particle sizes as measured by Ulysses for ISD from the LIC.

As the interstellar dust particles move through the heliosphere plasma, they emit electrons by photoionisation from the solar UV radiation. They also pick up electrons and protons from the solar wind and they emit electrons by secondary electron emission from energetic electrons and ions. These processes are in equilibrium and as a result, the particles have a more or less constant positive potential of typically  $U = +5$  V in interplanetary space because of the dominance of photoionisation (Grün and Landgraf, 2001) and because the plasma density as well as UV radiation intensity decline with the square of the distance to the Sun. In changing plasma environments, like close to the Sun ( $< 1$  AU), in planetary magnetospheres, or near the heliospheric boundary regions, the particles have different surface potentials and can have negative, or time-varying potentials (Slavin et al., 2012, Fig. 2). The smaller the particle, the larger its charge-to-mass ratio ( $Q/m$ ), and the more it is influenced by the Lorentz force. These particles are moving through the interplanetary

magnetic field with alternating sectors of positive and negative polarity, and hence, they are deflected by the Lorentz force in an alternating manner. The polarity of the interplanetary magnetic field depends on the solar cycle, and as a result the submicron-sized ISD particles are deflected away from the solar equatorial plane for a large part of the eleven-year solar cycle, and focused near the solar equatorial plane in the subsequent solar cycle.

Very small particles (smaller than about 0.01 micron) have a large charge-to-mass ratio and thus couple tightly to local magnetic fields. Therefore, they do not enter the heliosphere but are deflected at the heliosphere boundary (Slavin et al., 2012; Alexashov et al., 2016). However, these are not relevant for radar measurements. Particles larger than that can enter the heliosphere and may reach the Solar System. They are deflected towards or away from the equatorial plane by the Lorentz force, depending on the polarity of the local interplanetary magnetic field and their size (and hence, charge-to-mass ratio). Particles entering at low ecliptic latitudes, for instance those coming from the LIC, are more likely to reach the Solar System because they pass more alternating magnetic field polarities (assuming a Parker interplanetary magnetic field from Parker, 1958). If large particles are observed from higher latitudes than those which come from the LIC (for instance, as claimed by Taylor et al., 1994), there are not necessarily also smaller particles from these latitudes, because they may be deflected away by the Lorentz force as they pass through fewer alternating polarities of the magnetic field. Moreover, the Lorentz force would likely scatter their direction of arrival.

To summarise, the smallest particles’ trajectories are mostly influenced by the Lorentz force, while the largest (a few  $\mu\text{m}$  in radius) are mostly influenced by solar gravity. For the flux of large ISD, the relative velocity of the Earth with respect to the ISD inflow vector plays a major role, in addition to the gravitational focusing<sup>2</sup>. This flux modulation leads to variations in relative ISD speeds (with respect to Earth) from a few  $\text{km s}^{-1}$  to up to 60  $\text{km s}^{-1}$  for typical “big” Ulysses-type LIC-particles (1  $\mu\text{m}$  diameter), and the relative flow direction can vary over a full 360° (Strub et al., 2019). Larger particles with  $\beta$  close to zero (e.g., 10  $\mu\text{m}$  diameter) would have speeds relative to Earth from 19 to 79  $\text{km s}^{-1}$ . The fluctuations in total mass flux of ISD onto Earth are dominated by the biggest particles because these contain most of the total dust mass. They are mainly caused by the Earth’s relative motion with respect to the ISD, and by the yearly increase in local ISD number density when the Earth passes near the gravitational focusing region of the dust particles, downstream from the Sun with respect to the inflow direction (Strub et al., 2019).

For large particles (interstellar meteoroids, a few tens of microns) that are not coupled to the LIC and that come from other star systems, the velocity at which the particle (ejected from the other star system) arrives at the Earth is a superposition of its ejection velocity and the star’s velocity relative to the Sun. The local stellar velocity distribution ranges from 15–40  $\text{km s}^{-1}$  depending on the star’s spectral type (Dehnen and Binney, 1998). The particle ejection velocity depends on the source: Murray et al. (2004) found speeds of  $\sim 1$   $\text{km s}^{-1}$  for debris

<sup>2</sup> Of course, this is also important for small ISD, in addition to velocity effects from the Lorentz and radiation pressure forces.

disks containing gas giants,  $\sim 10 \text{ km s}^{-1}$  for Asymptotic Giant Branch (AGB) star dust ejection, and perhaps  $\sim 100 \text{ km s}^{-1}$  in collimated bipolar outflows from young stellar objects. In any case, the excess speed  $v_a$  at which the interstellar particle arrives at the edge of the Solar System might be tens of  $\text{km s}^{-1}$ .

The speed measured by a detector at Earth has the additional component resulting from the fall into the Sun's potential well. As a result, at the Earth a particle arriving with speed  $v_a$  will have a measured heliocentric speed  $v_H = \sqrt{42^2 + v_a^2}$ , which is  $49 \text{ km s}^{-1}$  (or  $7 \text{ km s}^{-1}$  above the parabolic velocity) for an arrival speed of  $25 \text{ km s}^{-1}$ . Interstellar meteors arriving from behind the Sun's motion with respect to the local standard of rest may of course arrive with almost zero excess velocity; typically, however, we expect them to arrive at Earth with speeds exceeding the Sun's escape speed by a few  $\text{km s}^{-1}$ . It is worth noting that meteoroids with hyperbolic speeds relative to the Sun will not necessarily have high speeds relative to the Earth. A particle on a hyperbolic orbit could arrive from behind our planet at a relative speed as low as  $12 \text{ km s}^{-1}$ , and in fact any sample of measured interstellar meteors should show a range of in-atmosphere speeds, not only high ones.

### 10.3 Hyperbolic Meteoroids Produced in the Solar System

It is possible for material on a bound orbit around our Sun to be transferred to a hyperbolic orbit. If this material should intersect with the Earth as it leaves the Solar System on its now-unbound orbit, it will appear as a hyperbolic meteor. However it is not of interstellar origin, and so these ejection processes must be understood in order to recognise true interstellar meteors.

Planetary perturbations can generate hyperbolic orbits from asteroidal or cometary particles through the slingshot effect (Lovell, 1954, Chapter XII; Öpik, 1969). These can occur when a planet encounters either sporadic meteoroids or a meteoroid stream. The later is relatively uncommon; however, Comet C/1995 O1 Hale-Bopp had a pre-perihelion encounter with Jupiter that could have scattered particles onto orbits reaching our planet at speeds almost  $1 \text{ km s}^{-1}$  above the parabolic velocity at Earth (Wiegert, 2014). Sporadic scattering is more common, but still relatively rare. Only one in 10 000 sporadics are expected to have been scattered to hyperbolic velocity by a planet (Wiegert, 2014). These originate mostly from Mercury and Venus, because of the higher dust densities and the abundance of meteoroids on nearly-unbound orbits there. However, these hyperbolic meteoroids are usually travelling only a few hundreds of meters per second above the heliocentric escape speed at Earth, and so such meteors are unlikely to be confused with interstellar meteors, as these are expected to have much higher heliocentric speeds.

Hyperbolic meteors can also be generated locally by solar radiation pressure. Particles with sufficiently large area-to-mass ratios find themselves in a state where the outward acceleration due to solar radiation pressure exceeds gravity, and they accelerate outwards. These are the "beta meteoroids" (Zook and Berg, 1975), typically less than 1 micron across, but their small sizes make them unlikely to be observed with traditional meteor techniques.

Comets approaching the Sun on highly eccentric orbits may release material onto hyperbolic orbits through outgassing processes. Though there is not one universally-accepted model for cometary ejection speeds (Whipple, 1950; Jones, 1995; Crifo, 1995; Ryabova, 2013) they are rarely expected to reach above  $1 \text{ km s}^{-1}$ , even near the Sun for comets with very low perihelia. Such meteoroids that reach the Earth will have slowed as they climb out of the Sun's gravitational well and are not likely to be misidentified as interstellar in origin.

Collisions between asteroids and impacts by meteoroids onto asteroid surfaces can release material onto unbound orbits. However, ejecta is usually released at speeds significantly below that of the impactor, making the process relatively inefficient. The ejecta velocity distribution is sensitive to the mechanical properties of the target and impactor (Waza et al., 1985), but ejection velocities are not observed above the impactor velocity. Random velocities in the asteroid belt are  $4\text{--}6 \text{ km s}^{-1}$  (Farinella and Davis, 1992; Bottke et al., 1994) while a  $\Delta v$  of  $7 \text{ km s}^{-1}$  is needed to put an asteroid on a near-circular orbit at 3 AU on a hyperbolic one; so asteroid collisions may in principle produce hyperbolic ejecta, but such events are rare.

Impacts by meteoroids into asteroid targets can occur at much higher relative velocities than inter-asteroid collisions, as the meteoroid environment contains a significant retrograde population, the apex meteoroids (Jones and Brown, 1993) thought to be derived from retrograde comets (Wiegert et al., 2009; Nesvorný et al., 2011). However, experiments show that meteoroid impacts typically produce relatively low ejection velocities, typically  $\sim 1\%$  of the impactor's (Braslau, 1970; Hartmann, 1985; Housen and Holsapple, 2011; Wiegert, 2015).

Planetary magnetic fields are known to accelerate charged particles. High-speed sub-micron grains were measured at Jupiter by the Ulysses spacecraft (Grün et al., 1993; Kempf et al., 2005) and were inferred to have originated from Io, become electrically charged in the Jovian plasma environment and accelerated by its magnetic field. Similar particles detected by the Cassini spacecraft at Saturn (Kempf et al., 2005) are thought to originate in Saturn's outer main ring. These small particles can be accelerated to very high speeds (larger than  $100 \text{ km s}^{-1}$ ) (Horanyi et al., 1993; Flandes et al., 2011).

### 10.4 Effect of Measurement Errors on the Resulting Orbit

Meteor observations, especially in the last two decades, are a rich data resource, extremely important for statistical evidence on the nature of the meteoroid orbits in the Solar System. However, the use of the orbits on an individual basis is very problematic and requires high-accuracy data to ensure that the resulting analyses are not biased by effects of measurement and determination errors. Discriminating between orbits of different natures for individual meteoroids is demanding, even for the most accurate photographic meteors (Kresák and Kresáková, 1976; Steel, 1996; Hughes and Williams, 2000).

In optical surveys, meteors are observed through visible light emitted during the ablation process, when meteoroids pass through the atmosphere. Measured parameters of a meteor (position and speed) are used to determine the orbit of the

meteoroid around the Sun. The orbital elements derived indicate the particles' origin. However, the semi-major axis  $a$ , which defines the type of the orbit, strongly depends upon the derived heliocentric velocity  $v_H$ , eventuating from the fundamental equation of the motion of a particle in the Sun's gravitational field:

$$v_H^2 = GM_S \left( \frac{2}{r} - \frac{1}{a} \right), \quad (10.1)$$

where  $r$  is the heliocentric distance (for the meteor observations in the Earth's atmosphere  $r \approx 1$  AU),  $M_S$  is the solar mass and  $G$  is the gravitational constant.

The determination of the heliocentric velocity  $v_H$  from photographic meteor observations proceeds in several steps involving various corrections (for atmospheric deceleration, diurnal aberration, acceleration by the Earth's gravitational field, and vector addition with the Earth's motion) (e.g. Kresák, 1992). Hence, the resulting value of  $v_H$ , determined, consequentially, from the measured speed  $v$ , the non-atmospheric velocity  $v_\infty$  and geocentric velocity  $v_G$ , is influenced by various errors: incorrect determination of the radiant, leading to incorrect heights and changing of the elongation of the radiant from the apex; errors in timing affecting the right ascension; difficulties with short meteor trail data reduction; changes in the rotation velocity of a sector or other errors arising from the equipment used. All these sources of uncertainty vary in importance, and cannot be easily separated from one another, but each of them tends to increase the inaccuracy of the determined values. At the end, the error of  $v_H$  can easily exceed  $1 \text{ km s}^{-1}$ . Such errors can transfer near-parabolic orbits over the parabolic limit and create an artificial population of hyperbolic meteors (Hajduková, 1994). The higher the velocity  $v_H$ , the smaller the error needed for this change.

This effect can be demonstrated by a diagram showing the correlation between the non-atmospheric velocity  $v_\infty$  (or geocentric velocity  $v_G$ ) and the angular elongation of the apparent radiant from the apex,  $\varepsilon_A$ . Based on Kresák and Kresáková (1976), we constructed, for different values of semi-major axis  $a$ , a diagram (Figure 10.2) showing the relation between these two quantities:

$$v_H^2 = v_G^2 + v_0^2 - 2v_G v_0 \cos \varepsilon_A, \quad (10.2)$$

where  $v_0$  is the mean heliocentric velocity of the Earth.

The diagram allows us to estimate the required measurement accuracy in speed and radiant position needed to discriminate between bound and unbound orbits. The required accuracy is different for different regions in the diagram, determined by the resolution within the particular area between individual orbits. The curves represent orbits with different values of semi-major axes (marked in the graph).

For the plot, we used rough data from the photographic catalogues of the Meteor Data Centre of the International Astronomical Union (IAU MDC), version 2003 (Lindblad et al., 2003). The database is created from more than fifteen different catalogues, each containing data obtained with different equipment and different determination software. Each of them differs in the proportion of hyperbolic orbits they contain, which raises concerns about the accuracy of their speed determinations. However, to reveal the sources of the inconsistencies is problematical.

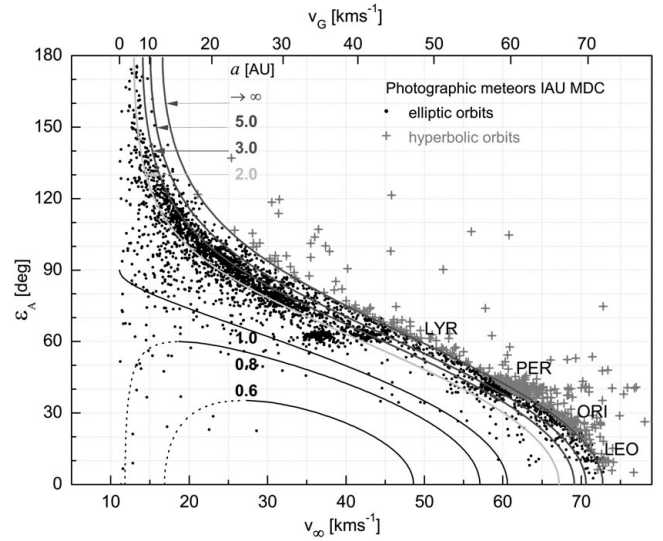


**Figure 10.2.** The effect of the measurement errors in radiant position and velocity on the resulting semi-major axis of the orbit. The angular elongation of the apparent radiant from the apex  $\varepsilon_A$  is plotted against the non-atmospheric velocity of meteors  $v_\infty$ , using rough photographic data of the IAU MDC (Lindblad et al., 2003) in which 11.5% of orbits were determined to be hyperbolic (crosses). The curves, representing the relation between  $\varepsilon_A$  and  $v_G$  according to Equation (10.2), are constructed for different values of semi-major axes  $a$ . (A black and white version of this figure will appear in some formats. For the colour version, please refer to the plate section.)

Of the 4581 meteors, 4054 meteors are on elliptic orbits (black circles) and 527 (11.5%) were determined by authors of the catalogues to be hyperbolic (crosses). These are beyond the parabolic limit in the right part of the diagram, in contrast to Kresák and Kresáková (1976), who used a sample of the most precise 413 Super-Schmidt meteor data (Jacchia and Whipple, 1961), leaving this part of the graph empty.

Due to the strong correlation between velocity and apex elongation, meteors are distributed in a very narrow zone of the diagram, where discriminating between orbits of different semi-major axes is most challenging (due to the resolution within this zone). It is clearly seen that for large  $a$ , the value of the semi-major axis derived is strongly affected by small errors in the measured speed or radiant position, especially for  $\varepsilon_A < 60$  deg. Following the example of Kresák and Kresáková (1976), discrimination between a long-period orbit and an orbit with its aphelion near Jupiter would demand a resolution better than  $\pm 3 \text{ km s}^{-1}$  in speed and  $\pm 5$  deg in radiant coordinates. The only regions of the diagram where a lower measuring accuracy would be sufficient is the lower left or upper right. The first area corresponds to orbits with aphelia near the Earth (in Figure 10.2, shown for semi-major axes of 0.6 and 0.8 AU). The dotted lines correspond to particles overtaken by the Earth and solid lines to the retrograde particles encountering the Earth head-on. The number of meteors in this area is low. The upper right region of the diagram corresponds to highly hyperbolic orbits, which are absent among the data investigated. There are few cases of high hyperbolic excesses in  $v_H$ ; however, they belong exclusively to the catalogues of lowest accuracy. The vast majority of

hyperbolic orbits in the diagram are concentrated in the line along the parabolic limit, where conditions are most demanding.

A detailed analysis of the same sample of the IAU MDC data (Hajduková, 2008) showed that the number of hyperbolic meteors in this sample does not in any case represent the number of interstellar meteors; the hyperbolicity of the vast majority of them is only apparent, caused by various errors. The upper limit of possible interstellar meteors in the data was statistically determined to be of the order of  $10^{-3}$ . The individual cases, however, cannot be identified as they are hidden within the error bars.

The first clear evidence of the influence of measurement errors, seen in Figure 10.2, is the concentration of shower meteors (the Perseids, Orionids, Lyrids and Leonids) among the hyperbolic orbits. These showers have known local sources, and so the presence of apparently hyperbolic orbits among them points to incorrect or insufficiently precise speed determination. To follow the influence of the errors on the sample of hyperbolic orbits, diagrams showing the position of radiant of orbits for the selected intervals of values of  $1/a$  close to the parabolic limit and beyond were constructed from various photographic and video data (Hajduková, 2008, 2011). In the case of true hyperbolic meteors, a gradual decrease in the concentration of shower radiants with decreasing values of  $1/a$  would be expected, but actually the opposite was found. Their concentration is higher among the orbits with the highest hyperbolic excesses, reaching a proportion of 1:1.

Moreover, analysis of hyperbolic shower meteors observed by different techniques showed that the proportion of hyperbolic orbits is different in different meteor showers. A clear dependence of the contribution of hyperbolic meteors in meteor showers on the mean heliocentric velocity of a particular shower ( $N_{e>1}/N = f(v_H)$ ) was found, which was true for the radio, photographic, and video data investigated (Hajduková, 2008, 2011). At any rate, these results and the assumption that the shower meteor orbits were determined with the same precision as non-shower data within the same catalogue, led Hajduková to conclude that there is a lack of statistical argument for the presence of meteors produced by interstellar particles observed in the Earth's atmosphere.

The disputability of hyperbolic shower meteors was noticed early by Fisher (1928) and Watson (1939), who pointed out the problem of over-estimation of the measured velocities leading to the artificial interstellar population. However, influenced by results of Hoffmeister and Öpik, the existence of interstellar meteor showers was seriously considered at that time.

Concerning hyperbolic shower meteors from radar surveys, Taylor et al. (1994) tested the very high velocity meteors observed by AMOR on the Eta Aquariid meteor shower. Approximately half of about 500 Eta Aquariids in their sample had hyperbolic orbits with  $a < 0$  and  $e > 1$ , with very extreme values of  $e = 1.5$ . This is a large fraction, yet perhaps not surprising, seeing that radio data require even more complicated treatment to yield the heliocentric orbital parameters (e.g. Šimek, 1966; Sekanina and Southworth, 1975; Taylor and Elford, 1998; Galligan and Baggaley, 2004) than is the case with photographic data reduction.

Meteor radars detect echoes from the ionisation produced by meteoroids entering the atmosphere and suffer from a number of

instrumental detection biases (see Chapter 3, Kero et al. 2019), such as the initial trail radius effect, the finite velocity effect, the pulse repetition factor, and Faraday rotation, described in detail in Moorhead et al. (2017). The increase in ionisation that occurs with increasing meteor speed is itself an observation bias that requires the largest correction to the speed distribution. Corrections to the observed radar speed distribution have been gradually improved by several authors, e.g. Taylor (1995) using the Harvard Radio Meteor Project (HRMP) data; Brown et al. (2004) using Canadian Meteor Orbit Radar (CMOR) data; Hunt et al. (2004), Close et al. (2007) analysing ALTAIR radar data; and Janches et al. (2014) using Arecibo observations. Recently, Moorhead et al. (2017) presented a method for correcting all the radar observation biases and applied it to the CMOR data. In spite of that, an unrealistically high fraction of seemingly hyperbolic meteors remained in their sample. They concluded that the uncertainty smoothing from the observed speed distribution has not yet been successfully deconvolved and that a thorough exploration of all sources of uncertainty and comparison of the results with other datasets and dynamical models is necessary (Moorhead et al., 2017).

In summary, we can conclude that to distinguish the detected interstellar particles from interplanetary ones is a significant challenge. Moreover, the expected hyperbolic excesses of a meteor's heliocentric velocity (see Section 10.2) are of the same order as the uncertainty in the velocity determination. This requires high-accuracy meteors and a proper error examination, failing which, each analysis using the velocity data will be seriously affected by measurement errors.

The following sections will show a review of studies related to interstellar meteoroids, each of which dealt with this problem to a greater or lesser degree.

## 10.5 Meteor Observations of Interstellar Particles

Searches for meteoroids of interstellar origin have been carried out using different observational techniques (photographic, image-intensified video and radar) as well as by data-mining for hyperbolic orbits in various meteor catalogues. Their detection, however, remains controversial. Here we summarise a portion of the relevant literature on the subject.

### 10.5.1 Optical Surveys

#### 10.5.1.1 Photographic

Photographic orbits from different catalogues of the IAU Meteor Data Centre (Lindblad, 1987) were analysed by Hajduková (1994), who determined an upper limit for possible interstellar particles of 0.02% for masses  $> 10^{-3}$  kg. Analysing the updated catalogues of the IAU MDC (Lindblad et al., 2001), Hajduková and Paulech (2002) concluded that the proportion of possible interstellar meteoroids in the mass range  $10^{-4}$ – $10^0$  kg does not exceed  $2.5 \times 10^{-4}$  of the total number of meteors. This value was used to set an upper limit for the flux of interstellar particles for the photographic mass interval,  $f_{ISP} < 10^{-18} \text{m}^{-2} \text{s}^{-1}$ , derived by the authors using the interplanetary particle distribution given by Divine et al. (1993).

### 10.5.1.2 Video

Hyperbolic meteors observed with video detectors were examined in several studies by Hawkes, Woodworth and their colleagues, who determined the contribution of interstellar meteoroids to the meteoroid population to be 1–2% for masses  $> 10^{-8}$  kg (Hawkes et al., 1999). The proportion of hyperbolic orbits in their data decreased from 6.5%, as reported in the first study (Hawkes et al., 1984), to 1.3%, when applying the 95% confidence limit (Hawkes and Woodworth, 1997a). After a comprehensive error analysis of 160 meteors, observed up to +8 magnitude by image-intensified video detectors, the authors announced the detection of two meteoroids, which arrived on high inclination orbits from interstellar space (Hawkes and Woodworth, 1997b). The two observed events were caused by particles of masses of the order of  $10^{-7}$  kg, with heliocentric velocities of  $49.9 \pm 1.7$  km s $^{-1}$  and  $48.4 \pm 0.6$  km s $^{-1}$ , respectively. Based on their analyses, the authors concluded that approximately 2% of the total meteoroid flux is interstellar in origin, and determined the flux of heliocentric hyperbolic meteoroids (at 1 AU) to be  $f_{ISP} = 1.3 \times 10^{-3}$  meteors, of mass greater than  $5 \times 10^{-8}$  kg, impacting a 100 m $^2$  detector per year (Hawkes et al., 1999).

An analysis based on a one-year survey for interstellar meteoroids using the Canadian Automated Meteor Observatory (CAMO), was reported by Musci et al. (2012). The two station automated electro-optical system detects meteors up to +5 magnitude with an average uncertainty of 1.5% in speed and about 0.4 deg in radiant direction. From a total of 1739 meteor orbits, the authors found 22 potential hyperbolic meteors; none of them had a heliocentric velocity greater than 45 km s $^{-1}$ . After a detailed examination and checking for close encounters with planets, the authors concluded that their few identified hyperbolic events are most likely the result of measurement errors. They determined an upper limit of the flux of interstellar meteoroids at Earth as  $f_{ISP} < 6 \times 10^{-14}$  m $^{-2}$ s $^{-1}$  and declared that they found no clear evidence of interstellar meteoroids with a limiting mass of  $m > 2 \times 10^{-7}$  kg.

Hyperbolic orbits from the SonotaCo catalogue (SonotaCo, 2009) and the European Video Meteor Network Database (EDMOND) (Kornoš et al., 2014) were analysed by Hajduková et al. (2014a,b); the hyperbolic excesses were in all cases very low and within the error bars. The flux of interstellar particles with a limiting mass  $m > 10^{-4}$  kg was estimated to be approximately  $f_{ISP} \sim 10^{-16}$  m $^{-2}$ s $^{-1}$ .

## 10.5.2 Radar Surveys

### 10.5.2.1 The AMOR Results

Significant contributions to the problem of hyperbolic meteors were made near the turn of the century in the work of Baggaley, Taylor, Bennett and others, based on observations from the Advanced Meteor Orbit Radar (Baggaley et al., 1993a; Baggaley and Bennett, 1996). This high-power radar system was located near Christchurch in New Zealand, and operated between 1990 and 2000, carrying out a survey of southern hemisphere radiants in order to determine the heliocentric orbits of the interplanetary dust and meteoroids that impact the Earth. The system sensitivity was +13 magnitude, corresponding to about 100  $\mu$ m-sized

particles, or to a mass limit of about  $10^{-9}$  kg (Baggaley et al., 1994). The fan-shaped radar antenna beam, narrow in azimuth yet broad in elevation, permitted a large declination response and hence a large ecliptic latitude sampling of the celestial sphere. Measuring a few  $10^3$  orbits daily, their data doubled the existing total database from all other orbit-measuring techniques at that time. For the first time, meteoroid orbits were determined using digitised raw data (Baggaley et al., 1993b). Orbital uncertainties (dependent on the meteors' atmospheric speed) were determined to be about 2 degrees in angular elements and about 5% in size elements (Baggaley, 2000).

The AMOR analyses yielded about 1% extremely hyperbolic orbits of meteoroids in the mass range of  $10^{-7}$ – $10^{-10}$  kg, with very high geocentric velocities in excess of 100 km s $^{-1}$  (Baggaley et al., 1993a; Taylor et al., 1994). This arbitrary limit was imposed to select values which are about five times the standard error above the parabolic limit and thus, well beyond the 3 sigma error. The velocities were derived from the time-lag values and from Verniani's ionisation relation (Verniani, 1973). The authors write about determined uncertainties of about 6 km s $^{-1}$  for a speed of  $v_G = 72$  km s $^{-1}$  (Baggaley et al., 1993a). The reality of the high-speed meteors was supported by their height distribution, which showed a peak 6–8 km higher than that for the full sample. Baggaley and his colleagues explained these very-high-velocity meteors as being produced by meteoroids on unbound orbits, and thus, they reported the detection of interstellar meteoroids in the Earth's atmosphere and presented a large sample of interstellar particles (Taylor et al., 1996; Baggaley, 1999). However, the authors did not provide any estimates of their flux.

One of the indicators of the meteors' interstellar origin were the directions of their heliocentric influx (Baggaley, 1999). Mapping the influx directions showed, other than a broad interstellar inflow (a high southern latitude open orbit component), the presence of discrete sources in the vicinity of the Sun (Baggaley and Galligan, 2001). Measuring a general background influx of extra-Solar System particles from southern ecliptic latitudes, the authors found enhanced areas. From intra-annual variations in the influx, they inferred the existence of discrete sources, one associated with the Sun's motion about the Galactic centre, and the other with the motion of the Solar System relative to nearby A-type stars (Taylor et al., 1996). The dominant compact directional inflow was believed to appear from the direction of the main-sequence debris-disk star  $\beta$  Pictoris (Baggaley, 2000). This was, however, questioned in a theoretical approach by Murray et al. (2004), who estimated that the observed particle flux coming from the discrete source observed by Baggaley (2000) is several orders of magnitude larger than would be expected from a debris disk at 20 pc. Moreover, the authors showed that the location of the source on the sky is inconsistent with particles ejected from  $\beta$  Pictoris.

The other indicator showing that the meteoroids are interstellar was the distribution of their orbital inclinations, which was found to be a clear function of the heliocentric velocity (Baggaley, 1999). For the closed orbit population, retrograde motion contributed about 5% of the meteors, whereas for the open orbits, this value rose to 41%. It has to be noted that the inclinations were derived using several corrections steps. Taking into account the observational bias effects, Galligan

and Baggaley (2002) described their analysis procedures and demonstrated the inclination distribution at successive levels of applied correction. They showed that about half of the directly observed inclination distributions was made up of progrades. This fraction was substantially over-represented due to ionisation efficiency, which increases with speed.

In any case, the analysis of the AMOR orbital data showed that the discrete features were present in all seasons within the year examined (Baggaley, 1999). The inclination distribution of those meteoroids that have a source direction exhibited clear seasonal changes, which, according to the author, can only be explained as being due to sources external to the Solar System. This was supported by a theoretical study by Baggaley and Neslušan (2002). Considering an influx of a collinear stream of interstellar particles (of sizes greater than 20  $\mu\text{m}$ ) into the Solar System, the authors modelled its evolution. The expected meteoroids at the Earth exhibited cyclic (seasonal) changes in the observed orbital elements. All elements, except for the inclination, depended on the dispersion of their original (far-Sun) speed; therefore, the variations in the inclination were most clearly discernible.

The reliability of the AMOR interstellar detections stands or falls on the reality of their extremely high velocities. The mean speed for the hyperbolic sample analysed in the paper (Taylor et al., 1996) was determined to be 164  $\text{km s}^{-1}$ , with an uncertainty of  $\pm 30 \text{ km s}^{-1}$ . In this paper, the authors outlined their statistical approach for confirmation of the high velocities, which was based on a comparison of the Fresnel and the time-lag determination (for the sample of meteors with lower velocities for which both methods were applied). Hajduk (2001) re-examined these methods and called attention to several contradictions; he concluded that the sets of highly hyperbolic velocities (in the range of 100–500  $\text{km s}^{-1}$ ) cannot be accepted unless an independent confirmation of the AMOR observational data is made. Recognising the limitations of the data is of high importance, since observations and orbital distributions are used as inputs in the modelling of the interplanetary dust population. The question whether these very high velocities are a consequence of a systematic error in the processing of the observations or not has not been proven as yet, although these high speeds have not been confirmed by other radar programs and observations.

The problem of meteors with high geocentric velocity and their connection to faint optical meteors at great heights was discussed by Woodworth and Hawkes (1996). The authors found no meteors with beginning heights greater than approximately 120 km, but argued that, because of the small field of view and the optimum intersection height assumed, they had an observational bias against high (and low) meteors. To reconcile their results with AMOR observations, the authors suggested several explanations: there could exist a flux of very fast and high meteors only at masses smaller than the limiting mass of their observations; or they could come from a radiant which strongly prefers southern hemisphere observers; or some constituent of the meteoroids could ablate at very great heights, producing ionisation but not luminosity. Or, on the other hand, the ionising efficiency, which might increase with velocity far more rapidly than the luminous efficiency factor, could bias radar results in favour of very fast meteors (Woodworth and Hawkes, 1996).

In two other works, Rogers et al. (2005), and extended in Hill et al. (2005), the authors modelled the heights, trail lengths and luminosities expected from high geocentric velocity meteor ablation in the Earth's atmosphere and suggested that very high velocity meteors (with entry masses larger than about  $10^{-8} \text{ kg}$ ) could, if they exist, be observed with current electro-optical technology, although there may be observational biases against their detection.

Moreover, the interstellar meteoroids detected by AMOR are also expected to be accompanied by a large number of even smaller grains, which, however, have not been detected by the space detectors on board the Ulysses and Galileo spacecrafts (Landgraf et al., 2000) which are sensitive in this size range, as Earth-bound detectors are not. Unless, as the authors speculated, the small grains have been stopped on their way to the Solar System by an interstellar cloud.

In spite of the controversy surrounding their highest velocity results and their applications, AMOR provided valuable information about the meteoroid population and contributed enormously to our understanding of the evolutionary processes of the small body dynamics.

#### 10.5.2.2 Other Radar Surveys

Using the Arecibo Observatory UHF Radar, Mathews et al. (1999) analysed thirty-two registered micrometeors (mass range of  $10^{-9}$ – $10^{-12} \text{ kg}$ ), fifteen of which were suitable for velocity determination. The velocities, determined by the direct Doppler method, were greater than the escape velocity for eleven of fifteen particles. In one case, the authors suggested it was of interstellar origin. The errors in the orbital elements were estimated by the authors (with several assumptions) to be 10% to 20%. (Janches et al., 2000). In their next study (Meisel et al., 2002a), 143 hyperbolic micrometeors were found in a set of 3000 particles showing measurable deceleration. The sample of hyperbolic orbits was analysed in detail and a final list of 108 interstellar particle candidates was presented. The authors, trying to establish the ISP origins, suggested they had arrived from the direction of the vicinity of the Geminga pulsar (Meisel et al., 2002b). However, according to Musci et al. (2012), they had assumed that all meteors came down the main beam and were not in one of the sidelobes. Moreover, meteors crossing the main beam come in at an angle that cannot be measured, meaning that only the radial velocity is truly known. This leads to large uncertainties in velocity. Thus, these Arecibo radar results remain disputed (Musci et al., 2012).

Radio data on meteoroids with a limiting mass of  $10^{-7} \text{ kg}$ , collected in the IAU Meteor Data Centre (Lindblad, 2003), were analysed by Hajduková (2008), with special emphasis on the 39145 orbits of the Harvard Radio Meteor Project. The examination indicated large errors in the velocity, reaching as much as  $10 \text{ km s}^{-1}$ . The author determined that only  $10^{-3}$  of the total number of Harvard radar orbits could be of interstellar origin. Other older radar meteors, observed by Meteor Automatic Radar System (MARS) in Kharkiv, were reanalysed by Kolomiyets (2015), who did not refute the reality of the MARS hyperbolic meteoroid orbits reported earlier (Andreev et al., 1987).

The Canadian Meteor Orbit Radar (CMOR) was also used in a search for interstellar meteors, conducted over 2.5 years by

Weryk and Brown (2004). CMOR is a interferometric HF/VHF meteor radar with a radio magnitude limit of +8, which corresponds to an effective limiting mass of  $4 \times 10^{-8}$  kg at typical interplanetary meteoroid encounter speeds (Jones et al., 2005). The system is used for time-of-flight velocity measurements and provides individual error estimates on all measured and derived quantities for each echo. Thus, the authors examined the data on a case-by-case basis for interstellar meteoroids (Weryk and Brown, 2004) and, when measurement errors were taken into account, they found only 12 meteors of possible interstellar origin among more than 1.5 million measured orbits. This corresponded to only 0.0008% of all the observed radar echoes. The authors determined a lower limit on the ISP flux at the Earth to be  $6 \times 10^{-15}$  meteoroids  $\text{m}^{-2} \text{s}^{-2}$  for the  $2\sigma$  criteria.

Meteor observations with the European Incoherent Scatter Scientific Association (EISCAT) radars were reported by Brosch et al. (2013). Examination of the statistical properties of the radar echoes and their Doppler velocity, derived from the VHF data, showed a lack of extreme velocity meteors. Considering only the meteors that encounter the Earth head-on, the authors reported no incoming velocities measured above  $72 \text{ km s}^{-1}$  and indicated that interstellar meteors are extremely rare. This confirmed previous observations by the EISCAT UHF (Szasz et al., 2008), in which, after all corrections have been made, only 4 of the 410 detected meteors had heliocentric velocities slightly exceeding the Solar System escape velocity. The authors did not claim their interstellar origin because the hyperbolic excesses were smaller than the uncertainties of the data treatment.

### 10.5.3 II/'Oumuamua

The discovery of the first macroscopic interstellar object II/'Oumuamua (Meech et al., 2017) opens the door to the study of interstellar fireballs in the Earth's atmosphere, though none have been reported to date. An order of magnitude estimate based on the single detected object II/'Oumuamua can be obtained, though its reliability is perhaps not very high. II was detected at 0.22 AU from Earth: so if we assume that one interstellar object of size 100 m (approximate average diameter of II, Knight et al. (2017)) passes through this Earth-centred cross-section ( $\sim 10^{15} \text{ km}^2$ ) every 10 years (the time PanSTARRS has been observing) then there should cumulatively be  $N(D > 10 \text{ cm}) \sim \left(\frac{0.1 \text{ m}}{100 \text{ m}}\right)^{-p+1}$  times more objects at sizes down to 10 cm, where  $p$  is the assumed slope of the differential size distribution. Adopting  $p = 3.5$  from the canonical paper of Dohnanyi (1969) gives  $\sim 0.1$  interstellars of 10 cm striking the Earth per year. If 50% strike during the day, and 70% over the oceans, we might expect only one at night over land per several decades. This low rate can likely be accommodated within current observational constraints from all-sky meteor networks but needs much more careful analysis.

## 10.6 In-Situ Measurements of Interstellar Dust

### 10.6.1 In-Situ Measurements

Predictions of interstellar dust entering the Solar System were made by Bertaux and Blamont (1976). Levy and Jokipii (1976)

recognised the role of the Lorentz force herein. Interstellar dust trajectories in the heliosphere were studied by Gustafson and Misconi (1979) and Morfill and Grün (1979) with a focus on the effects of the Lorentz force. Finally, in 1992, the first interstellar dust impacts were detected in situ on a dust instrument on board the Ulysses mission (Grün et al., 1993). Ulysses flew out of the ecliptic plane, which facilitated the reliable detection of interstellar dust particles amongst the interplanetary dust population (see Section 10.6.3). The mission lasted from 1990 until 2009 and the ISD data cover a time-span from 1992 to 2008.

A similar (twin) instrument flew on Galileo from 1989 until 2003 towards and around Jupiter. It confirmed the measurements of interstellar dust made by Ulysses, but *in* the ecliptic plane and during its cruise phase (Baguhl et al., 1996). Reliable identification of these particles was only possible outside of the asteroid belt because of the geometry of the Galileo spacecraft trajectory.

Landgraf et al. (2000) performed Monte Carlo simulations of interstellar dust trajectories in the heliosphere (without boundary regions) and compared these with the Ulysses measurements available then. The depletion seen for the smallest particles could not be justified by instrument sensitivity alone, but was best explained by the effect of the Lorentz force, using the simulations. For the radiation pressure-mass relation, the  $\beta$ -curve for "astronomical silicates" was used from Gustafson (1994) with corresponding dust bulk material density of  $2.5 \text{ g cm}^{-3}$ . With these assumptions, a best fit was found between data and simulations for ISD particles with size  $0.3 \mu\text{m}$  (bulk population),  $0.4 \mu\text{m}$ , and to a lesser extent  $0.2 \mu\text{m}$  (Landgraf et al., 2003). The Ulysses data, supported by these simulations, thus confirmed the early predictions from studies like Morfill and Grün (1979). Landgraf et al. (1999) also constrained the optical dust properties ( $\beta$ -values) from the Ulysses ISD measurements by analyzing the spatial distribution of the particles with respect to their mass. This is called "*interstellar dust  $\beta$ -spectroscopy*" (Altobelli et al., 2005). Landgraf et al. (1999) concluded that the maximum  $\beta$ -value of the dust particles as measured by Ulysses is between 1.4 and 1.8. Follow-up simulation studies (e.g. Sterken et al. 2012) used this maximum value in the so-called "adapted astronomical silicate"  $\beta$ -curve. This is the original curve from Gustafson (1994) multiplied to reach a maximum of  $\beta = 1.6$ .

Cassini carried an impact ionisation dust detector (the *Cassini Cosmic Dust Analyser*) that was equipped with a high rate detector and a time-of-flight (TOF) mass spectrometer (Srama et al., 2004). During the cruise phase to Saturn, interstellar dust was identified inside the Earth's orbit (Altobelli et al., 2003) for the first time. The fluxes were consistent with simultaneous ISD measurements at Ulysses. The measured mass range was between  $5 \times 10^{-17} \text{ kg}$  and  $10^{-15} \text{ kg}$ , proving that both small and larger (about  $1 \mu\text{m}$  diameter) interstellar dust can also reach the inner Solar System. Altobelli et al. (2005) expanded the earlier Galileo data analysis of Baguhl et al. (1996) by using new selection criteria, which allowed studying ISD impacts down to 0.7 AU, including "*ISD  $\beta$ -spectroscopy*".

Helios data allowed further analysis of ISD near the Earth between 0.3 and 1 AU from the Sun (Altobelli et al., 2006) and provided the first mass spectra of the particles using a time-of-flight mass spectrometer (mass resolution:  $\frac{M}{\Delta m} \approx 5$  Altobelli

et al., 2006). The results indicated compositions compatible with silicates, and a mix of various minerals were present in the data.

Krüger et al. (2007) reported on a shift in latitude of the direction from which the interstellar dust particles came, as measured by Ulysses in 2005. The cause of this was unknown.

The Stardust mission was launched in 1999 and captured cometary dust on one side of a collector consisting of aerogel tiles, while the other side was used to capture interstellar dust particles. This was done at speeds as low as possible (a few  $\text{km s}^{-1}$ ) in order to capture the particles as intact as possible. The interstellar dust was collected between approximately 1 and 2 AU, during two specific periods in 2000 and 2002, totalling 195 days (Westphal et al., 2014). The collector was brought back to Earth in 2006, after which the tiles were cut and then scanned under an automatic microscope. These images were made available on the Internet for lay people to search for the particles after some initial online training. This was a successful example of citizen-science. Three interstellar dust candidates were found in the aerogel tiles, and another four craters from presumably interstellar impacts (with remnants) were found in the aluminum foils that surround the tiles. The particles were very diverse in (crystal) structure, composition and size, and particularly surprising was the low density of the candidates in the aerogel (Westphal et al., 2014).

The complete Ulysses dataset from 1992 until 2008 was finally analysed for ISD by Krüger et al. (2015) for the mass distribution, by Strub et al. (2015) for the flux and variability, and by Sterken et al. (2015) for the interpretation of the data using Monte Carlo computer simulations. This dataset totalled more than 900 selected ISD particles spanning three quarters of a Hale cycle. The flux of ISD in the Solar System as measured during these sixteen years of operations was on average  $7 \times 10^{-5} \text{ m}^{-2} \text{ s}^{-1}$ , with fluctuations from about  $1 \times 10^{-5} \text{ m}^{-2} \text{ s}^{-1}$  to almost  $2 \times 10^{-4} \text{ m}^{-2} \text{ s}^{-1}$  (Strub et al., 2015). The bulk of the particles had masses between  $10^{-17}$  and  $10^{-16}$  kg (Krüger et al., 2015) with minima and maxima of about  $10^{-18}$  kg and  $1.7 \times 10^{-14}$  kg (equivalent to 0.1 and 2.3  $\mu\text{m}$  diameter assuming bulk material densities of  $2.5 \text{ g cm}^{-3}$ ).

The reanalysis of the Ulysses ISD data from 1992 until about 2000 by Krüger et al. (2015); Strub et al. (2015); Sterken et al. (2015) confirmed the earlier results from studies by Landgraf et al. (2000). The shift in dust flow direction as shown by Krüger et al. (2007) could possibly be explained with the simulations using dust properties of charge-to-mass ratio  $Q/m \approx 4 \text{ C/kg}$ , but if these would be the bulk of the dust particles, then the fluxes in the first period of Ulysses observations would have been larger, which was not the case. It is likely that the shift in dust flow direction (latitude) for these particles is due to Lorentz forces and not dynamics outside of the heliosphere, but a single fit of the simulations to all the data at once (1992–2008) remains to be found in order to prove and confirm this proposed mechanism. This also would imply that the “big” particles ( $> 0.2 \mu\text{m}$ ) in the Ulysses data are fluffy rather than compact, because for these masses a lower  $Q/m$  would have been expected (Sterken et al., 2015).

Since one single dominant dust size or population (characterised by one set of  $\beta$  and  $Q/m$ ) cannot explain the full sixteen years of data, Sterken et al. (2015) speculated that the heliosphere boundary plays an extra role in the filtering of ISD

on its way to the Solar System. Full simulations, including boundary regions of the heliosphere, are probably necessary to find one fit for all the data at once. The study suggests that big particles are possibly fluffy while smaller ones may be more compact.

The Cassini Dust Analyser TOF mass spectrometer detected interstellar particles during Cassini’s mission around Saturn. In a timespan from mid-2004 until 2013, thirty-six particles were identified as interstellar. Due to sensitivity limits of the instrument, only particles from  $10^{-19}$  to  $5 \times 10^{-16}$  kg were in the range of masses that could be analysed. The dust composition was rather homogenous, implying repeated processing of the dust in the interstellar medium (Altobelli et al., 2016). The dust consisted of magnesium-rich silicate particles, some with iron inclusions (Altobelli et al., 2016). The derived  $\beta$ -curve was rather compatible with compact particles, unlike their larger counterparts from the Stardust and Ulysses missions.

Several spacecraft (e.g. Voyager, Gurnett et al., 1983) have detected dust impacts using plasma wave instruments (antennas) that pick up a signal from the small plasma cloud that arises temporarily after a dust impact on the spacecraft body. So far, two missions have detected  $\sim 1 \mu\text{m}$  impacts of dust with a yearly variation in the flux that is compatible with the direction of the flow of interstellar dust from the LIC in the Solar System. These are the STEREO and WIND missions (Zaslavsky et al., 2012; Malaspina et al., 2014), both in the vicinity of the Earth (1 AU). The WIND mission’s twenty-two years of interstellar dust measurements (1994–2016) have been archived in a database for future use (Malaspina and Wilson, 2016). The data partially overlap the Ulysses data (1994–2008) and span a full Hale cycle.

### 10.6.2 Impact Ionisation Instruments, Laboratory Calibrations and Instrument Limitations

The Ulysses Dust Analyser instrument is a typical impact ionisation detector with a maximum sensitive area of  $0.1 \text{ m}^2$  and an effective solid angle of  $1.45 \text{ sr}^3$  (corresponding to a  $140^\circ$  opening angle, Baguhl et al., 1996). It is sensitive to dust particles of masses between about  $10^{-19}$  and  $10^{-9}$  kg, but this sensitivity is speed-dependent (see, e.g., figure 8 in Grün et al. 1992). For impact speeds of  $40 \text{ km s}^{-1}$ , the measurement limits are  $10^{-19} \text{ kg} < m < 10^{-13} \text{ kg}$  and for impact speeds of  $5 \text{ km s}^{-1}$ , the limits are  $10^{-16} \text{ kg} < m < 10^{-10} \text{ kg}$  (Grün et al., 1992). Above this mass, the instrument works as a threshold detector (Grün et al., 1992) and is saturated, while below this mass the instrument sensitivity is not high enough to reliably detect an impact. This means that such an instrument in an orbit near the Earth would be sensitive to different parts of the interstellar dust mass distribution depending on the time of the year. Instrument calibrations were performed using iron, carbon and silicates (Goeller and Grün, 1989). The Cassini instrument has similar characteristics, and calibrations have been performed for a larger variety of materials. Fielding et al. (2015) present a comprehensive review of these materials (e.g. Polypyrrole-coated mineral grains).

<sup>3</sup> A flat plate has an “effective solid angle” of  $\pi \text{ sr}$  (Goeller and Grün, 1989).

The measurement principle is based on impact ionisation: when dust particles with velocities larger than about  $1 \text{ km s}^{-1}$  hit the gold-coated spherical target of the instrument, the dust particle and part of the target vaporises and ionises. The ions and electrons are separated by the electric field applied between the target (0 V for Ulysses) and the ion collector ( $-350 \text{ V}$  for Ulysses). The speed of the impacting particle is estimated using the rise-time of the signal while the mass is estimated based on the velocity and the total charge in the plasma cloud after impact:  $Q \approx m^\alpha v^\gamma$  with  $\alpha \approx 1$  and  $\gamma \approx 1.5\text{--}5.5$  depending on the speed range. Krüger et al. (2015) used calibration curves from Grün et al. (1995) for the reduction of the sixteen years of Ulysses ISD data. The speed is determined with an accuracy of typically a factor of 2 (using only one channel) resulting in an accuracy of a factor of 10 for the mass (Grün et al., 1992). Because of the large uncertainty in the speed determination, Landgraf et al. (2000) and Krüger et al. (2015) have obtained more reliable results for the ISD mass distributions using simulated velocities instead of measured in order to determine the measured masses. Apart from dust impact velocity and mass, the instrument also measures impact direction as inferred from its pointing direction on the spinning spacecraft. The electric charge of the largest particles is also measured through the induction on an entrance grid, but only for very large particles (Grün et al., 1992; Krüger et al., 2015).

### 10.6.3 ISD Selection Criteria

The orbit of Ulysses largely facilitated the distinction of interstellar dust from interplanetary dust because it was more or less perpendicular to the inflow direction of the ISD from the LIC: only at perihelion would the ISD come from the same (prograde) direction as the IDPs, while during the rest of the orbit, ISD would rather come from the retrograde direction with respect to Ulysses, and opposite to most of the IDPs. In addition, Ulysses flew out of the ecliptic plane, where IDPs are much less present than in the ecliptic plane where distinguishing IDPs from ISD is a lot more challenging (e.g. during the Galileo mission). While Krüger et al. (2015) focused on the mass distribution of ISD and therefore did not select on impact charge signal, Strub et al. (2015) avoided biases in the directionality of the dust flow and selected particles based on impact velocity. The following selection criteria were used for the analysis of sixteen years of Ulysses data:

- Impacts were distinguished from noise events using instrument-specific procedures (see Krüger et al., 2015).
- Both Krüger et al. (2015) and Strub et al. (2015) excluded all data during intervals of Jupiter dust stream periods as well as around perihelion (latitudes  $|b| < 60^\circ$ ).
- Krüger et al. (2015) excluded data at ecliptic latitudes larger than  $60^\circ$  near perihelion where the ion charge signal  $Q_I \leq 10^{-13} \text{ C}$ . These were considered to be  $\beta$ -meteoroids.
- Krüger et al. (2015) required the instrument to point within  $\pm 90^\circ$  from the interstellar Helium upstream direction, except in 2005/2006, where this requirement was relaxed with another  $40^\circ$  (in one direction) to account for the shift in dust flow direction that was observed.

- Strub et al. (2015) ignored all impacts with  $Q_I \leq 1 \times 10^{-13} \text{ C}$  (Jupiter dust streams, in addition to the periods mentioned in previous points).
- Strub et al. (2015) ignored all impacts with speeds  $V_{imp} \leq 11.6 \text{ km s}^{-1}$  to exclude interplanetary dust that has lower velocities than interstellar dust.

The selection of Krüger et al. (2015) resulted in a dataset of 987 particles, while the selection of Strub et al. (2015) resulted in a dataset of 580 particles.

## 10.7 Summary

The Solar System is not an isolated system. Its interaction with the interstellar medium, due to the Sun's motion relative to the local interstellar cloud (LIC), should lead to the presence of interstellar particles (ISP), or, at least, to interstellar dust (ISD). Interstellar grains passing through the Solar System have been observed by dust detectors. Cassini, Ulysses, Helios and Galileo all had impact ionisation detectors that provided coherent numbers for the ISD flux throughout the Solar System and throughout time for a mass range of about  $10^{-19}\text{--}10^{-13} \text{ kg}$ . The upper limit of the mass range is limited by instrument saturation, and by the smaller number of large particles in the size distribution that could hit an instrument surface area of only  $0.1 \text{ m}^2$ . The lowest-mass-particle measurements are limited because of instrument sensitivity (speed-dependent) and the filtering of small particles due to the Lorentz force. Impact measurements on spacecraft with antennas like WIND and STEREO provide useful long-term monitoring possibilities for ISD particles in addition to dedicated cosmic dust detectors.

The situation with the interstellar meteoroids observed in the Earth's atmosphere is not so clear. On a theoretical basis, it was shown that particles larger than about  $10 \text{ }\mu\text{m}$  can travel tens of parsecs through the interstellar medium (Murray et al., 2004), theoretically creating the possibility of their detection by ground-based radar systems. Measurements of them have not yet been satisfactorily convincing.

Owing to the limitations of the accuracy of current meteor measurements, distinguishing interstellar particles from local meteoroids is very challenging. Hence, their proportion among interplanetary meteors has not yet been unambiguously determined, though it seems to increase strongly with decreasing particle mass. The reported derived fluxes of ISPs observed by different techniques (Sections 10.5.1, 10.5.2 and 10.6.1) are synthesised in several studies, and summarised in this section. Determination of the fluxes of interstellar particles obtained from different surveys allows the mass indices for a broad scale of masses to be derived and provides a comprehensive perspective. The reported ISP fluxes from various papers were recently compiled by Musci et al. (2012). Since no new studies reporting the detection of interstellar meteoroids have been published since that time, we use their figure to give an overview of interstellar particles detected to date. Their examination of the literature is summarised in Figure 10.3.

Figure 10.3 shows the fluxes for ISPs in a broad mass range, exceeding 20 orders of magnitude, with scales showing the approximate sensitivity for different detectors. The reported

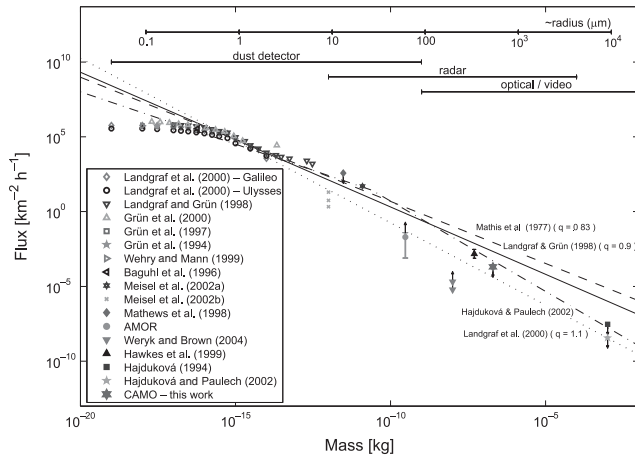


**Figure 10.3.** A summary of the interstellar meteoroid fluxes from the literature, from Musci et al. (2012). Different symbols designate primary sources of interstellar data. The lines in different styles represent the modelled mass distributions or those fitted by power-law functions determined by different authors. (A black and white version of this figure will appear in some formats. For the colour version, please refer to the plate section.)

detections of ISPs are shown with different symbols designating primary data sources.

The fluxes of the ISD data used in Figure 10.3 are based on Landgraf and Grün (1998) and Landgraf et al. (2000), who analysed the Ulysses and Galileo data. In contradiction to their modelled mass distributions (solid and dotted lines), the measured flux of the smallest grains (for masses  $< 10^{-16}$  kg) showed a deficiency. This was explained by defocusing Lorentz forces, which kept the smaller interstellar particles out of the heliosphere (Baguhl et al., 1996). On the other side, the flux of big interstellar grains from dust detectors was overestimated when using the measured impact velocities. The authors attributed it to possible mis-identification of interplanetary particles (the interstellar data set may be contaminated by interplanetary grains) or to systematic deviation of the measured impact velocity to lower values. Therefore, for the mass distribution determination, calculated values were used instead of measured velocities. This resulted in an increase in the number of small grains ( $m < 10^{-16}$  kg) and a decrease in the number of large grains ( $m > 10^{-16}$  kg).

Landgraf et al. (2000) extrapolated the dust data to larger masses by fitting a power law function (with the exponent  $q = 1.1$ , dotted line in Figure 10.3) and compared them with the fluxes derived from the AMOR radar measurements (for meteoroids with  $m > 10^{-10}$  kg). The authors concluded that these two samples are not kinematically related to each other. From the radar data, only one source (interstellar particles coming from the same direction as the dust detectors data) was compatible with the extrapolation of the in situ data; the fluxes of the other two directions examined (from the southern ecliptic hemisphere and from a discrete source) were one or two orders of magnitude larger.

Hajduková and Paulech (2002) summarised ISP fluxes obtained from observations with different techniques for particles masses from  $10^{-20}$  to  $10^{-2}$  kg and compared the

resulting ISP flux (dash-dotted line in Figure 10.3) with the flux model of interplanetary particles suggested by Fechtig (1973). When determining the mass distributions, the authors obtained different mass indices for two different mass intervals, matching the break at masses between  $10^{-10}$  and  $10^{-11}$  suggested by Fechtig (1973). The distribution was steeper for larger particles (with an exponent in the power-law fit of  $q \sim 1.2$ , as estimated by Musci et al. (2012)), and shallower for smaller particles ( $q \sim 0.7$ ).

Comparison of the ISP flux with another flux model derived by Grün et al. (1985), which gives slightly higher fluxes than derived by Fechtig (1973), also implies an increasing proportion of the ISPs toward smaller masses.

Hajduková and Hajduk (2006), following the summarised experimental data, obtained a smooth change of the curve of the mass distribution for ISPs. The substantial change in the integrated mass distribution indices was, however, also in the mass interval corresponding to the break seen in previous studies. Comparison of their resulting ISP flux with the interplanetary flux model by Divine (1993) showed that the ISP flux is more than two orders of magnitude lower than the flux of interplanetary meteoroids in the mass range of large particles, but strongly increases towards fainter particles.

To match spacecraft dust measurements, new models were developed that consider the population of hyperbolic orbits of dust particles, which is predicted to disappear for larger masses (Staubach et al., 1997; Dikarev et al., 2002).

In Figure 10.3, no comparison of the mass distributions of the ISPs with interplanetary flux models is shown. But they are compared with the size distribution of interstellar grains from the observed interstellar extinction, derived for masses below  $10^{-15}$  kg by Mathis et al. (1977). Musci et al. (2012) extended it to larger particles (dashed line in Figure 10.3) and found that the resulting flux derived from CAMO data (and other optical and radar data in this mass range) is clearly below it, which means that the slope for larger masses has to be much steeper.

We can conclude that in spite of the relatively large number of hyperbolic orbits determined from the meteor observations by Earth-based systems, at most only a fraction could be expected to be produced by interstellar particles. However, none of them have yet been convincingly demonstrated and their presence among detected meteors lacks statistical significance. The only dependable measured interstellar particles in our Solar System which we have to date are the detections of the dust instruments, mainly on board Ulysses and Galileo spacecraft.

## 10.8 Future Work

Research into interstellar particles has, for decades, brought controversial results, mostly due to meteor observations being misinterpreted as indicating the detection of interstellar meteoroids. This paper shows that the identification of meteors produced by interstellar particles requires an understanding of their dynamical behaviour, highly accurate measurements, and a thorough error examination. Hence, without any improvements to the velocity measurements, which are crucial for orbit determination, the problem of distinguishing interstellar meteors from interplanetary ones remains.

Earth-based and space-borne observations use different techniques with different instrumental sensitivities, and the data processing is performed using different software. In addition, there are obvious constraints related to the heliocentric distance of the measurements, and their latitude and speed. The instruments for meteor observations in the Earth's atmosphere move at a heliocentric velocity of about  $29.8 \text{ km s}^{-1}$ , in comparison with the dust detectors, where this value varies for individual spacecraft.

Thus, each individual observation gives us some information while still leaving gaps in the data between different techniques, and together they gradually reveal the population of interstellar particles in the Solar System.

Missions with detectors out of the ecliptic plane, long-term monitoring, as well as missions far from the Sun (e.g., 10 AU for reaching particles with  $\beta \approx 5$ ) are important tools to constrain interstellar dust properties. Space-borne instruments with trajectory sensors would allow better orbit determination of the ISD. The most interesting would be to be able to bridge the gap between particle sizes observed by in-situ instruments (up to about  $5 \mu\text{m}$ ) and those observable by radar and optical technologies (typically as from a few tens of  $\mu\text{m}$ ). Large surface areas, long exposure times, high-precision directional information, high-precision velocity determination, and sensitivity to the largest/smallest particles (for space/Earth instruments respectively) would be characteristics needed for an instrument<sup>4</sup> targeted at detecting these intermediate-range interstellar dust particles. Current selection criteria may also exclude interstellar dust particles that come from different directions than from the solar apex direction, and thus dust from sources other than the LIC.

Improvements in ground-based radar systems should allow the detection of interstellar meteoroids in the 10–100-micrometer range (Murray et al., 2004). This would make it possible to register interstellar particles ejected from other star systems. The forthcoming radar system EISCAT 3D (Pellinen-Wannberg et al., 2016) seems promising for registering even smaller particles (with a limiting mass of  $10^{-12} \text{ kg}$ ).

To prove the existence of meteoroids with very high geocentric velocities, search strategies need also to be optimised. Modelling the atmospheric ablation and the luminosity of meteoroids with geocentric velocities, Rogers et al. (2005) suggested improvements to electro-optical technology: using several multi-station observing systems with slightly overlapping fields to create a large net field of view; and, to avoid the observational bias due to the optimum intersection, the system configuration of an altitude of 120 km is required.

Experimental approaches, as made by Thomas et al. (2016) measuring the ionisation efficiency of meteors (up to  $70 \text{ km s}^{-1}$ ) and high-altitude ablation in the laboratory, could also cast light on this problem.

So far, the focus of interstellar dust trajectory modelling has been mainly on the effects of the dynamic IMF, solar radiation pressure and gravity on the particle trajectories within 50 AU from the Sun. Static models were also used of the whole heliosphere (Slavin et al., 2012), but they do not yet

represent the ISD distribution in the Solar System, because the ISD travels for more than 20 years (2 solar cycles) through a dynamic heliosphere. Alexashov et al. (2016) focused on the distribution of the dust outside of the Heliopause, based on a 3D kinetic-magnetohydrodynamics model of the solar wind-Local Interstellar Medium (LISM) interaction. Understanding the trajectories of ISD particles smaller than half a micron in diameter (“interstellar dust”) requires the inclusion of the (dynamic) outer heliosphere regions in the currently existing dynamic dust-heliosphere models of interplanetary space (Sterken et al., 2015). Data of the ISD flux and flow direction, taken by Ulysses between 1992 and 2008, can constrain such models.

In 2017, the first interstellar asteroid II/“*Oumuamua*” was discovered with a hyperbolic trajectory around the Sun. An abundance of at least  $6.0 \times 10^{-3} \text{ AU}^{-3}$  was estimated for such objects in interstellar space (Feng and Jones, 2018). A continuous mass distribution of interstellar objects (meteoroids, dust particles) is thus very likely present in the interstellar medium. Backtracking is difficult for individual objects due to gravitational scattering from random stellar encounters (Zhang, 2018) and because of the limitations of current astrometry, but for younger objects, this may be possible. The discovery of this interstellar asteroid sheds new light on the possible existence of interstellar meteoroids and shows the importance of closing the gap between measurements of interstellar dust particles with in-situ data, and the ground-based methods for their larger counterparts.

## Acknowledgements

This work was supported by the Natural Sciences and Engineering Research Council of Canada, grant No. RGPIN-2018-05659, by the Slovak Scientific Grant Agency, grant No. VEGA 2/0037/18, and by the Slovak Research and Development Agency, contract No. APVV-16-0148.

## References

- Alexashov, D. B., Katushkina, O. A., Izmodenov, V. V., and Akaev, P. S. 2016. Interstellar dust distribution outside the heliopause: Deflection at the heliospheric interface. *Monthly Notices of the Royal Astronomical Society*, **458**, 2553–2564.
- Almond, M., Davies, J. G., and Lovell, A. C. B. 1953. The velocity distribution of sporadic meteors. IV. Extension to magnitude + 8, and final conclusions. *Monthly Notices of the Royal Astronomical Society*, **113**, 411–427.
- Altobelli, N. 2004 (May). *Monitoring of the Interstellar Dust Stream in the Inner Solar System Using Data of Different Spacecraft*. Ph.D. thesis, Ruprecht-Karls-Universität Heidelberg.
- Altobelli, N., Kempf, S., Landgraf, M. et al. 2003. Cassini between Venus and Earth: Detection of interstellar dust. *Journal of Geophysical Research (Space Physics)*, **108**, 8032.
- Altobelli, N., Kempf, S., Krüger, H. et al. 2005. Interstellar dust flux measurements by the Galileo dust instrument between the orbits of Venus and Mars. *Journal of Geophysical Research (Space Physics)*, **110**, A07102.
- Altobelli, N., Grün, E., and Landgraf, M. 2006. A new look into the Helios dust experiment data: presence of interstellar dust inside the Earth's orbit. *Astronomy & Astrophysics*, **448**, 243–252.

<sup>4</sup> Also called a Swiss army knife.

- Altobelli, N., Postberg, F., Fiege, K. et al. 2016. Flux and composition of interstellar dust at Saturn from Cassini's Cosmic Dust Analyzer. *Science*, **352**, 312–318.
- Andreev, G. V., Kashcheev, B. L., and Kolomiets, S. V. 1987. Contradictions of the problem of hyperbolic meteors. *Meteornye Issledovaniia*, **13**, 93–104.
- Baggaley, J., and Galligan, D. 2001. Monitoring the near-space meteoroid population using the AMOR Radar Facility. In: H. Sawaya-Lacoste (ed.), *Proceedings of the Third European Conference on Space Debris, 19 - 21 March 2001, Darmstadt, Germany*, pp. 219–221. ESA SP-473, Vol. 1, Noordwijk, Netherlands: ESA Publications Division, ISBN 92-9092-733-X, 2001.
- Baggaley, J. W., and Bennett, R. G. T. 1996. The Meteoroid Orbit Facility Amor: Recent Developments. Pages 65–70 of: Gustafson, B. Å. S., and Hanner, M. S. (eds), *IAU Colloq. 150: Physics, Chemistry, and Dynamics of Interplanetary Dust*, Gainesville, FL, 14–18 August 1995. [Astronomical Society of the Pacific Conference Series, vol. 104]. San Francisco: Astronomical Society of the Pacific.
- Baggaley, W. J. 1999. The interstellar particle component measured by AMOR. Pages 265–273 of: Baggaley, W. J., and Porubcan, V. (eds), *Meteoroids 1998*. Bratislava: Astronomical Institute of the Slovak Academy of Sciences
- Baggaley, W. J. 2000. Advanced Meteor Orbit Radar observations of interstellar meteoroids. *Journal of Geophysical Research*, **105**, 10353–10362.
- Baggaley, W. J., and Neslušan, L. 2002. A model of the heliocentric orbits of a stream of Earth-impacting interstellar meteoroids. *Astronomy & Astrophysics*, **382**, 1118–1124.
- Baggaley, W. J., Taylor, A. D., and Steel, D. I. 1993a. The influx of meteoroids with hyperbolic heliocentric orbits. Pages 53–56 of: Stohl, J., and Williams, I. P. (eds), *Meteoroids and their Parent Bodies*, Smolenice, Slovakia, July 6–12, 1992. Bratislava: Astronomical Institute, Slovak Academy of Sciences.
- Baggaley, W. J., Taylor, A. D., and Steel, D. I. 1993b. The southern hemisphere meteor orbit radar facility: AMOR. Pages 245–248 of: Stohl, J., and Williams, I. P. (eds), *Meteoroids and their Parent Bodies*, Smolenice, Slovakia, July 6–12, 1992. Bratislava: Astronomical Institute, Slovak Academy of Sciences.
- Baggaley, W. J., Bennett, R. G. T., Steel, D. I., and Taylor, A. D. 1994. The Advanced Meteor Orbit Radar Facility: AMOR. *Quarterly Journal of the Royal Astronomical Society*, **35**, 293–320.
- Baguhl, M., Grün, E., Linkert, G., Linkert, D., and Siddique, N. 1993. Identification of “small” dust impacts in the Ulysses dust detector data: Relevance to Jupiter dust streams Page 1036 of: *AAS/Division for Planetary Sciences Meeting Abstracts #25*. Bulletin of the American Astronomical Society, vol. 25.
- Baguhl, M., Grün, E., and Landgraf, M. 1996. In situ measurements of interstellar dust with the ULYSSES and Galileo spaceprobes. *Space Science Reviews*, **78**, 165–172.
- Bertaux, J. L., and Blamont, J. E. 1976. Possible evidence for penetration of interstellar dust into the solar system. *Nature*, **262**, 263–266.
- Bottke, W. F., Nolan, M. C., Greenberg, R., and Kolvoord, R. A. 1994. Velocity distributions among colliding asteroids. *Icarus*, **107**, 255–268.
- Braslau, D. 1970. Partitioning of energy in hypervelocity impact against loose sand targets. *Journal of Geophysical Research*, **75**, 3987–3999.
- Brosch, N., Häggström, I., and Pellinen-Wannberg, A. 2013. EISCAT observations of meteors from the sporadic complex. *Monthly Notices of the Royal Astronomical Society*, **434**, 2907–2921.
- Brown, P., Jones, J., Weryk, R. J., and Campbell-Brown, M. D. 2004. The velocity distribution of meteoroids at the Earth as measured by the Canadian Meteor Orbit Radar (CMOR). *Earth, Moon, and Planets*, **95**, 617–626.
- Close, S., Brown, P., Campbell-Brown, M., Oppenheim, M., and Colestock, P. 2007. Meteor head echo radar data: Mass-velocity selection effects. *Icarus*, **186**, 547–556.
- Crifo, J. F. 1995. A general physicochemical model of the inner coma of active comets. 1: Implications of spatially distributed gas and dust production. *The Astrophysical Journal*, **445**, 470–488.
- Dehnen, W., and Binney, J. J. 1998. Local stellar kinematics from HIPPARCOS data. *Monthly Notices of the Royal Astronomical Society*, **298**, 387–394.
- Dikarev, V., Jehn, R., and Grün, E. 2002. Towards a new model of the interplanetary meteoroid environment. *Advances in Space Research*, **29**, 1171–1175.
- Divine, N. 1993. Five populations of interplanetary meteoroids. *Journal of Geophysical Research*, **98**, 17029–17048.
- Dohnanyi, J. S. 1969. Collisional model of asteroids and their debris. *Journal of Geophysical Research*, **74**, 2531–2554.
- Draine, B. T., and Lee, H. M. 1984. Optical properties of interstellar graphite and silicate grains. *The Astrophysical Journal*, **285**, 89–108.
- Farinella, P., and Davis, D. R. 1992. Collision rates and impact velocities in the Main Asteroid Belt. *Icarus*, **97**, 111–123.
- Fechtig, H. 1973. Cosmic dust in the atmosphere and in the interplanetary space at 1 AU today and in the early Solar System Pages 209–221 of: Hemenway, C. L., Millman, P. M., and Cook, A. F. (eds), *Evolutionary and Physical Properties of Meteoroids*. National Aeronautics and Space Administration SP, vol. 319. State University of New York, Albany, NY, June 14–17. Washington: NASA
- Feng, F., and Jones, H. R. A. 2018. Oumuamua as a messenger from the local association. *The Astrophysical Journal*, **852**, L27.
- Fielding, Lee A., Hillier, Jon K., Burchell, Mark J., and Armes, Steven P. 2015. Space science applications for conducting polymer particles: Synthetic mimics for cosmic dust and micrometeorites. *Chemical Communications*, **51**, 16886–16899.
- Fisher, W. J. 1928. Remarks on the Fireball Catalogue of von Niessl and Hoffmeister. *Harvard College Observatory Circular*, **331**, 1–8.
- Flandes, A., Krüger, H., Hamilton, D. P. et al. 2011. Magnetic field modulated dust streams from Jupiter in interplanetary space. *Planetary and Space Science*, **59**, 1455–1471.
- Frisch, P. C., Dorschner, J. M., Geiss, J. et al. 1999. Dust in the local interstellar wind. *The Astrophysical Journal*, **525**, 492–516.
- Galligan, D. P., and Baggaley, W. J. 2002. The meteoroid orbital distribution at 1 AU determined by Amor. Pages 225–228 of: Warmbein, B. (ed), *Asteroids, Comets, and Meteors—ACM 2002 International Conference*, 29 July–2 August 2002, Berlin, Germany. Ed. Barbara Warmbein. ESA SP–500. Noordwijk, Netherlands: ESA Publications Division, ISBN 92-9092-810-7.
- Galligan, D. P., and Baggaley, W. J. 2004. The orbital distribution of radar-detected meteoroids of the Solar system dust cloud. *Monthly Notices of the Royal Astronomical Society*, **353**, 422–446.
- Goeller, J. R., and Grün, E. 1989. Calibration of the Galileo/Ulysses dust detectors with different projectile materials and at varying impact angles. *Planetary and Space Science*, **37**, 1197–1206.
- Grün, E., and Landgraf, M. 2000. Collisional consequences of big interstellar grains. *Journal of Geophysical Research*, **105**, 10291–10298.
- Grün, E., and Landgraf, M. 2001. Fast dust in the heliosphere. *Space Science Reviews*, **99**, 151–164.
- Grün, E., and Svestka, J. 1996. Physics of interplanetary and interstellar Dust. *Space Science Reviews*, **78**, 347–360.
- Grun, E., Zook, H. A., Fechtig, H., and Giese, R. H. 1985. Collisional balance of the meteoritic complex. *Icarus*, **62**, 244–272.

- Grün, E., Fechtig, H., Kissel, J. et al. 1992. The ULYSSES dust experiment. *Astronomy & Astrophysics Supplement*, **92**, 411–423.
- Grün, E., Zook, H. A., Baguhl, M. et al. 1993. Discovery of Jovian dust streams and interstellar grains by the ULYSSES spacecraft. *Nature*, **362**, 428–430.
- Grün, E., Baguhl, M., Hamilton, D. P. et al. 1995. Reduction of Galileo and Ulysses dust data. *Planetary and Space Science*, **43**, 941–951.
- Gurnett, D. A., Grun, E., Gallagher, D., Kurth, W. S., and Scarf, F. L. 1983. Micron-sized particles detected near Saturn by the Voyager plasma wave instrument. *Icarus*, **53**, 236–254.
- Gustafson, B. A. S. 1994. Physics of Zodiacal Dust. *Annual Review of Earth and Planetary Sciences*, **22**, 553–595.
- Gustafson, B. A. S., and Misconi, N. Y. 1979. Streaming of interstellar grains in the solar system. *Nature*, **282**, 276–278.
- Hajduk, A. 2001. On the very high velocity meteors. Pages 557–559 of: Warmbein, B. (ed), *Meteoroids 2001 Conference*. ESA Special Publication, vol. 495, 6–10 August 2001, Swedish Institute for Space Physics, Kiruna, Sweden. ESTEC, Noordwijk, the Netherlands.
- Hajduková, M. Jr. 1993. On the hyperbolic and interstellar meteor orbits. Pages 61–64 of: Stohl, J., and Williams, I. P. (eds), *Meteoroids and their Parent Bodies*. Bratislava: Astronomical Institute of the Slovak Academy of Sciences.
- Hajduková, M. Jr. 1994. On the frequency of interstellar meteoroids. *Astronomy & Astrophysics*, **288**, 330–334.
- Hajduková, M. 2008. Meteors in the IAU Meteor Data Center on Hyperbolic Orbits. *Earth, Moon, and Planets*, **102**, 67–71.
- Hajduková, M. Jr. 2011. Interstellar meteoroids in the Japanese tv catalogue. *Publications of the Astronomical Society of Japan*, **63**, 481–487.
- Hajduková, M. Jr. and Hajduk, A. 2006. Mass distribution of interstellar and interplanetary particles. *Contributions of the Astronomical Observatory Skalnaté Pleso*, **36**, 15–25.
- Hajduková, M. Jr. and Paulech, T. 2002. Interstellar and interplanetary meteoroid flux from updated IAU MDC data. Pages 173–176 of: Warmbein, B. (ed), *Asteroids, Comets, and Meteors – ACM 2002 International Conference*, 29 July – 2 August 2002, Berlin, Germany. ESA SP–500. Noordwijk, Netherlands: ESA Publications Division, ISBN 92-9092-810-7.
- Hajduková, M., Kornoš, L., and Tóth, J. 2014a. Frequency of hyperbolic and interstellar meteoroids. *Meteoritics and Planetary Science*, **49**, 63–68.
- Hajduková, M. Jr., Kornoš, L., and Tóth, J. 2014b. Hyperbolic Orbits in the EDMOND. Pages 289–295 of: Jopek, T.J., Rietmeijer, F.J., Watanabe, M. J., and Williams, I.P. (eds), *Proceedings of the Meteoroids 2013*. Poznan: Adam Mickiewicz University Press.
- Hartmann, W. K. 1985. Impact experiments. I - Ejecta velocity distributions and related results from regolith targets. *Icarus*, **63**, 69–98.
- Hawkes, R. L., and Woodworth, S. C. 1997a. Do some meteorites come from interstellar space? *Journal of the Royal Astronomical Society of Canada*, **91**, 68–73.
- Hawkes, R. L., and Woodworth, S. C. 1997b. Optical detection of two meteoroids from interstellar space. *Journal of the Royal Astronomical Society of Canada*, **91**(Oct.), 218–219.
- Hawkes, R. L., Jones, J., and Ceplecha, Z. 1984. The populations and orbits of double-station TV meteors. *Bulletin of the Astronomical Institutes of Czechoslovakia*, **35**, 46–64.
- Hawkes, R. L., Close, T., and Woodworth, S. 1999. Meteoroids from outside the Solar System. Pages 257–264 of: Baggaley, W. J., and Porubcan, V. (eds), *Meteoroids 1998*. Bratislava: Astronomical Institute of the Slovak Academy of Sciences.
- Hill, K. A., Rogers, L. A., and Hawkes, R. L. 2005. High geocentric velocity meteor ablation. *Astronomy & Astrophysics*, **444**, 615–624.
- Horanyi, M., Morfill, G., and Grun, E. 1993. Mechanism for the acceleration and ejection of dust grains from Jupiter's magnetosphere. *Nature*, **363**, 144–146.
- Housen, K. R., and Holsapple, K. A. 2011. Ejecta from impact craters. *Icarus*, **211**, 856–875.
- Hughes, D. W., and Williams, I. P. 2000. The velocity distributions of periodic comets and stream meteoroids. *Monthly Notices of the Royal Astronomical Society*, **315**, 629–634.
- Hunt, S. M., Oppenheim, M., Close, S. et al. 2004. Determination of the meteoroid velocity distribution at the Earth using high-gain radar. *Icarus*, **168**, 34–42.
- Jacchia, L. G., and Whipple, F. L. 1961. Precision orbits of 413 photographic meteors. *Smithsonian Contributions to Astrophysics*, **4**, 97–129.
- Janches, D., Mathews, J. D., Meisel, D. D., Getman, V. S., and Zhou, Q.-H. 2000. Doppler studies of Near-Antapex UHF radar micrometeors. *Icarus*, **143**, 347–353.
- Janches, D., Plane, J. M. C., Nesvorný, D. et al. 2014. Radar detectability studies of slow and small zodiacal dust cloud particles. I. The case of Arecibo 430 MHz meteor head echo observations. *The Astrophysical Journal*, **796**, 41.
- Jones, J. 1995. The ejection of meteoroids from comets. *Monthly Notices of the Royal Astronomical Society*, **275**, 773–780.
- Jones, J., and Brown, P. 1993. Sporadic meteor radiant distributions - Orbital survey results. *Monthly Notices of the Royal Astronomical Society*, **265**, 524–532.
- Jones, J., Brown, P., Ellis, K. J. et al. 2005. The Canadian Meteor Orbit Radar: System overview and preliminary results. *Planetary and Space Science*, **53**, 413–421.
- Kempf, S., Srama, R., Horányi, M. et al. 2005. High-velocity streams of dust originating from Saturn. *Nature*, **433**, 289–291.
- Kero, J., Campbell-Brown, M., Stober, G. et al. 2019. Radar observations of meteors. In: G. O. Ryabova, D. J. Asher, and M. D. Campbell-Brown (eds), *Meteoroids: Sources of Meteors on Earth and Beyond*. Cambridge, UK: Cambridge University Press, pp. 65–89.
- Kimura, H., and Mann, I. 1999. Radiation pressure on porous micrometeoroids. Pages 283–286 of: Baggaley, W. J., and Porubcan, V. (eds), *Meteoroids 1998*. Bratislava: Astronomical Institute of the Slovak Academy of Sciences.
- Knight, M. M., Protopapa, S., Kelley, M. S. P. et al. 2017. On the rotation period and shape of the hyperbolic asteroid II/\*Oumuamua (2017 U1) from its lightcurve. *The Astrophysical Journal*, **851**, L31.
- Kolomiyyets, S. V. 2015. Uncertainties in MARS meteor Orbit radar data. *Journal of Atmospheric and Solar-Terrestrial Physics*, **124**, 21–29.
- Kornoš, L., Koukal, J., Piffel, R., and Tóth, J. 2014. EDMOND Meteor Database. Pages 23–25 of: Gyssens, M., Roggemans, P., and Zoladek, P. (eds), *Proceedings of the International Meteor Conference, Poznan, Poland, 22–25 August 2013*. Hove, Belgium; IMO.
- Kresák, L. 1992. On the ejection and dispersion velocities of meteor particles. *Contributions of the Astronomical Observatory Skalnaté Pleso*, **22**, 123–130.
- Kresák, L., and Kresáková, M. 1976. A note on meteor and micrometeoroid orbits determined from rough velocity data. *Bulletin of the Astronomical Institutes of Czechoslovakia*, **27**, 106–109.
- Krüger, H., Landgraf, M., Altobelli, N., and Grün, E. 2007. Interstellar dust in the Solar System. *Space Science Reviews*, **130**, 401–408.
- Krüger, H., Strub, P., Grün, E., and Sterken, V. J. 2015. Sixteen years of Ulysses interstellar dust measurements in the Solar System. I. Mass distribution and gas-to-dust mass ratio. *The Astrophysical Journal*, **812**, 139.
- Landgraf, M. 2000. Modeling the motion and distribution of interstellar dust inside the heliosphere. *Journal of Geophysical Research*, **105**, 10303–10316.

- Landgraf, M., and Grün, E. 1998. In Situ Measurements of Interstellar Dust. Pages 381–384 of: Breitschwerdt, D., Freyberg, M. J., and Truemper, J. (eds), *IAU Colloq. 166: The Local Bubble and Beyond*. Lecture Notes in Physics, Berlin: Springer Verlag, vol. 506.
- Landgraf, M., Augustsson, K., Grün, E., and Gustafson, B. Å. S. 1999. Deflection of the local interstellar dust flow by solar radiation pressure. *Science*, **286**, 2319–2322.
- Landgraf, M., Baggaley, W. J., Grün, E., Krüger, H., and Linkert, G. 2000. Aspects of the mass distribution of interstellar dust grains in the solar system from in situ measurements. *Journal of Geophysical Research*, **105**, 10343–10352.
- Landgraf, M., Krüger, H., Altobelli, N., and Grün, E. 2003. Penetration of the heliosphere by the interstellar dust stream during solar maximum. *Journal of Geophysical Research (Space Physics)*, **108**, 8030.
- Levy, E. H., and Jokipii, J. R. 1976. Penetration of interstellar dust into the solar system. *Nature*, **264**, 423–424.
- Lindblad, B. A. 1987. The IAU Meteor Data Center in Lund. *Publications of the Astronomical Institute of the Czechoslovak Academy of Sciences*, **67**, 201–204.
- Lindblad, B. A. 2003. Private Communication.
- Lindblad, B. A., Neslušan, L., Svoreň, J., and Porubčan, V. 2001. The updated version of the IAU MDC database of photographic meteor orbits. Pages 73–75 of: Warmbein, B. (ed), *Meteoroids 2001 Conference*. ESA Special Publication, vol. 495, 6–10 August 2001, Swedish Institute for Space Physics, Kiruna, Sweden. ESTEC, Noordwijk, the Netherlands.
- Lindblad, B. A., Neslušan, L., Porubčan, V., and Svoreň, J. 2003. IAU Meteor Database of photographic orbits version 2003. *Earth, Moon, and Planets*, **93**, 249–260.
- Linde, T. J., and Gombosi, T. I. 2000. Interstellar dust filtration at the heliospheric interface. *Journal of Geophysical Research*, **105**, 10411–10418.
- Lovell, A. C. B. 1954. *Meteor Astronomy*. Oxford: Clarendon Press.
- Malaspina, D. M., and Wilson, L. B. 2016. A database of interplanetary and interstellar dust detected by the Wind spacecraft. *Journal of Geophysical Research (Space Physics)*, **121**, 9369–9377.
- Malaspina, D. M., Horányi, M., Zaslavsky, A. et al. 2014. Interplanetary and interstellar dust observed by the Wind/WAVES electric field instrument. *Geophysical Research Letters*, **41**, 266–272.
- Mathews, J. D., Meisel, D. D., Janches, D., Getman, V. S., and Zhou, Q.-H. 1999. Possible origins of low inclination antapex micrometeoroids observed using the Arecibo UHF radar. Pages 79–82 of: Baggaley, W. J., and Porubčan, V. (eds), *Meteoroids 1998*. Bratislava: Astronomical Institute of the Slovak Academy of Sciences.
- Mathis, J. S., Rumpl, W., and Nordsieck, K. H. 1977. The size distribution of interstellar grains. *The Astrophysical Journal*, **217**, 425–433.
- McKinley, D. W. R. 1951. Meteor velocities determined by radio observations. *The Astrophysical Journal*, **113**, 225–267.
- Meech, K. J., Weryk, R., Micheli, M. et al. 2017. A brief visit from a red and extremely elongated interstellar asteroid. *Nature*, **552**, 378–381.
- Meisel, D. D., Janches, D., and Mathews, J. D. 2002a. Extrasolar micrometeoroids radiating from the vicinity of the local interstellar bubble. *The Astrophysical Journal*, **567**, 323–341.
- Meisel, D. D., Janches, D., and Mathews, J. D. 2002b. The size distribution of arecibo interstellar particles and its implications. *The Astrophysical Journal*, **579**, 895–904.
- Moorhead, A. V., Brown, P. G., Campbell-Brown, M. D., Heynen, D., and Cooke, W. J. 2017. Fully correcting the meteor speed distribution for radar observing biases. *Planetary and Space Science*, **143**, 209–217.
- Morfill, G. E., and Grün, E. 1979. The motion of charged dust particles in interplanetary space - II. Interstellar grains. *Planetary and Space Science*, **27**, 1283–1292.
- Murray, N., Weingartner, J. C., and Capobianco, C. 2004. On the flux of extrasolar dust in Earth's atmosphere. *The Astrophysical Journal*, **600**, 804–827.
- Musci, R., Weryk, R. J., Brown, P., Campbell-Brown, M. D., and Wiegert, P. A. 2012. An optical survey for millimeter-sized interstellar meteoroids. *The Astrophysical Journal*, **745**, 161.
- Nesvorný, D., Vokrouhlický, D., Pokorný, P., and Janches, D. 2011. Dynamics of dust particles released from Oort Cloud comets and their contribution to radar meteors. *The Astrophysical Journal*, **743**, 37.
- Öpik, E. 1940. Meteors (Council report on the progress of astronomy). *Monthly Notices of the Royal Astronomical Society*, **100**, 315–326.
- Öpik, E. J. 1950. Interstellar meteors and related problems. *Irish Astronomical Journal*, **1**, 80–96.
- Öpik, E. J. 1969. NEWS AND COMMENTS- Interstellar Meteors. *Irish Astronomical Journal*, **9**, 156–159.
- Parker, E. N. 1958. Dynamics of the interplanetary gas and magnetic fields. *The Astrophysical Journal*, **128**, 664–676.
- Pellinen-Wannberg, A., Kero, J., Häggström, I., Mann, I., and Tjulin, A. 2016. The forthcoming EISCAT\_3D as an extra-terrestrial matter monitor. *Planetary and Space Science*, **123**, 33–40.
- Porter, J. G. 1944. An analysis of British meteor data: Part 2, Analysis. *Monthly Notices of the Royal Astronomical Society*, **104**, 257–271.
- Rogers, L. A., Hill, K. A., and Hawkes, R. L. 2005. Mass loss due to sputtering and thermal processes in meteoroid ablation. *Planetary and Space Science*, **53**, 1341–1354.
- Ryabova, G. O. 2013. Modeling of meteoroid streams: The velocity of ejection of meteoroids from comets (a review). *Solar System Research*, **47**, 219–238.
- Sarma, T., and Jones, J. 1985. Double-station observations of 454 TV meteors. I - Trajectories. *Bulletin of the Astronomical Institutes of Czechoslovakia*, **36**, 9–24.
- Sekanina, Z., and Southworth, R. B. 1975. *Physical and dynamical studies of meteors. Meteor-fragmentation and stream-distribution studies*. NASA CR 2615. Cambridge, MA: Smithsonian Institution.
- Šimek, M. 1966. Some errors in determining meteor velocities by the diffraction method. *Bulletin of the Astronomical Institutes of Czechoslovakia*, **17**, 90–92.
- Slavin, J. D., Frisch, P. C., Müller, H.-R. et al. 2012. Trajectories and distribution of interstellar dust grains in the heliosphere. *The Astrophysical Journal*, **760**, 46.
- SonotaCo. 2009. A meteor shower catalog based on video observations in 2007–2008. *WGN, Journal of the International Meteor Organization*, **37**, 55–62.
- Srama, R., Ahrens, T. J., Altobelli, N. et al. 2004. The Cassini Cosmic Dust Analyzer. *Space Science Reviews*, **114**, 465–518.
- Staubach, P., Grün, E., and Jehn, R. 1997. The meteoroid environment near Earth. *Advances in Space Research*, **19**, 301–308.
- Steel, D. 1996. Meteoroid orbits. *Space Science Reviews*, **78**, 507–553.
- Sterken, V. J., Altobelli, N., Kempf, S. et al. 2012. The flow of interstellar dust into the solar system. *Astronomy & Astrophysics*, **538**, A102.
- Sterken, V. J., Strub, P., Krüger, H., von Steiger, R., and Frisch, P. 2015. Sixteen years of Ulysses interstellar dust measurements in the Solar System. III. Simulations and data unveil new insights into local interstellar dust. *The Astrophysical Journal*, **812**, 141.
- Štohl, J. 1970. On the problem of hyperbolic meteors. *Bulletin of the Astronomical Institutes of Czechoslovakia*, **21**, 10–17.
- Strub, P., Krüger, H., and Sterken, V. J. 2015. Sixteen years of Ulysses interstellar dust measurements in the Solar System. II. Fluctuations

- in the dust flow from the data. *The Astrophysical Journal*, **812**, 140.
- Strub, P., Sterken, V.J., Soja, R. et al. 2019. Heliospheric modulation of the interstellar dust flow on to Earth. *Astronomy & Astrophysics*, **621**, A54.
- Szasz, C., Kero, J., Meisel, D. D. et al. 2008. Orbit characteristics of the tristatic EISCAT UHF meteors. *Monthly Notices of the Royal Astronomical Society*, **388**, 15–25.
- Taylor, A. D. 1995. The Harvard Radio Meteor Project meteor velocity distribution reappraised. *Icarus*, **116**, 154–158.
- Taylor, A. D., and Elford, W. G. 1998. Meteoroid orbital element distributions at 1 AU deduced from the Harvard Radio Meteor Project observations. *Earth, Planets, and Space*, **50**, 569–575.
- Taylor, A. D., Baggaley, W. J., Bennett, R. G. T., and Steel, D. I. 1994. Radar measurements of very high velocity meteors with AMOR. *Planetary and Space Science*, **42**, 135–140.
- Taylor, A. D., Baggaley, W. J., and Steel, D. I. 1996. Discovery of interstellar dust entering the Earth's atmosphere. *Nature*, **380**, 323–325.
- Thomas, E., Horányi, M., Janches, D. et al. 2016. Measurements of the ionization coefficient of simulated iron micrometeoroids. *Geophysical Research Letters*, **43**, 3645–3652.
- Tkachuk, A. A., and Kolomiets, S. V. 1985. The distribution of angular elements in the near-parabolic and near-hyperbolic orbits of meteoric bodies. *Meteornye Issledovaniia*, **10**, 67–74.
- Verniani, F. 1973. An analysis of the physical parameters of 5759 Faint Radio Meteors. *Journal of Geophysical Research*, **78**, 8429–8462.
- Von Niebl, G., and Hoffmeister, C. 1925. *Katalog der Bestimmungsgrößen für 611 Bahnen großer Meteore*. Vol. 100. Wien: Denkschriften der Akademie der Wissenschaft. Mathematisch-Naturwissenschaftliche Klasse.
- Watson, Fletcher. 1939. A study of fireball radiant positions. *Proceedings of the American Philosophical Society*, **81**(4), 473–479.
- Waza, T., Matsui, T., and Kani, K. 1985. Laboratory simulation of planetesimal collision: 2. Ejecta velocity distribution. *Journal of Geophysical Research: Solid Earth*, **90**(B2), 1995–2011.
- Weryk, R. J., and Brown, P. 2004. A search for interstellar meteoroids using the Canadian Meteor Orbit Radar (CMOR). *Earth, Moon, and Planets*, **95**, 221–227.
- Westphal, A. J., Stroud, R. M., Bechtel, H. A. et al. 2014. Evidence for interstellar origin of seven dust particles collected by the Stardust spacecraft. *Science*, **345**, 786–791.
- Whipple, F. L. 1940. Photographics meteor studies. III. The Taurid shower. *Proceedings of the American Philosophical Society*, **83**, 711–745.
- Whipple, F. L. 1950. A comet model. I. The acceleration of comet Encke. *The Astrophysical Journal*, **111**, 375–394.
- Wiegert, P., Vaubaillon, J., and Campbell-Brown, M. 2009. A dynamical model of the sporadic meteoroid complex. *Icarus*, **201**, 295–310.
- Wiegert, P. A. 2014. Hyperbolic meteors: Interstellar or generated locally via the gravitational slingshot effect? *Icarus*, **242**, 112–121.
- Wiegert, P. A. 2015. Meteoroid impacts onto asteroids: A competitor for Yarkovsky and YORP. *Icarus*, **252**, 22–31.
- Woodworth, S. C., and Hawkes, R. L. 1996. Optical Search for High Meteors in Hyperbolic Orbits. Pages 83–86 of: Gustafson, B. Å. S., and Hanner, M. S. (eds), *Physics, Chemistry, and Dynamics of Interplanetary Dust*. Proceedings of the 150th colloquium of the International Astronomical Union held in Gainesville, Florida, USA 14–18 August 1995. [Astronomical Society of the Pacific Conference Series, vol. 104]. San Francisco: Astronomical Society of the Pacific.
- Zaslavsky, A., Meyer-Vernet, N., Mann, I. et al. 2012. Interplanetary dust detection by radio antennas: Mass calibration and fluxes measured by STEREO/WAVES. *Journal of Geophysical Research (Space Physics)*, **117**, A05102.
- Zhang, Q. 2018. Prospects for backtracing 1I/Oumuamua and future interstellar objects. *The Astrophysical Journal*, **852**, L13.
- Zook, H. A., and Berg, O. E. 1975. A source for hyperbolic cosmic dust particles. *Planetary and Space Science*, **23**, 183–203.